ANL-AFCI-091

Physics study of the TRADE: TRIGA Accelerator Driven Experiment

D. G. Naberejnev[1], G. Imel[2], G. Palmiotti[1], M. Salvatores[1]

[1] *Nuclear Engineering Division , Argonne National Laboratory*
[2] *Nuclear Technology Division, Argonne National Laboratory*

Argonne National Laboratory
9700 S. Cass Avenue
Argonne, IL, 60439, USA

September 2003

Physics study of the TRADE: TRIGA Accelerator Driven Experiment

D. G. Naberejnev[1], G. Imel[2], G. Palmiotti[1], M. Salvatores[1]

[1] *Nuclear Engineering Division , Argonne National Laboratory*
[2] *Nuclear Technology Division, Argonne National Laboratory*

Abstract

This report deals with the validation of an ADS dynamic behaviour through the TRADE program. We first describe the motivations behind the TRADE project. This includes the types of ADS experiments to be performed and their necessity, beam trips issues, representativity of the experiment, and steps to be taken in the validation procedure. Then we perform the characterization of the TRADE core using deterministic methods. The general core description is given. A number of results related to the core criticality and modeling with different geometries are presented. Finally we report the experimental results of the recent critical measurements including the control rod calibration, determination of the critical configurations and fluxes in the core.

Table of content

Table of figures

I. Introduction

In principle three different level of validation of an ADS have been specified.

First, validation of the different component concepts, taken separately (accelerator, target, subcritical core, dedicated fuels and fuel processing methods).

Second, validation of the coupling of the different components in a significant environment, e.g. in terms of power of the global installation, using as far as possible existing critical reactors, to be adapted to the objectives.

Third, validation in an installation explicitly designed for demonstration (e.g. the ADS installation described in the European roadmap). This third step should evolve to a demonstration of transmutation fuels, after a first phase in which the subcritical core is loaded with "standard" fuel.

This report deals with the first and second validation levels. In the first chapter, we consider the motivations behind the TRADE project. This includes the types of ADS experiments to be performed and their necessity, beam trips issues, representativity of the experiment, and steps to be taken in the validation procedure. The second chapter addresses the characterization of the TRADE core using deterministic methods. The general core description is given. A number of results related to the core criticality and modeling with different geometries are presented. The last chapter reports the experimental results of the recent critical measurements including the control rod calibration, determination of the critical configurations and fluxes in the core.

II. Overview of motivations and work scope behind TRADE project

II.1 Introduction

As pointed out in the previous chapter and Ref. 1, three different level of validation of an ADS can be identified. The TRADE (TRIGA Accelerator Driven Experiment) program represents one of the most significant steps towards the ADS demonstration, in particular dealing with the second level of the ADS validation. The main purpose of this chapter is to emphasize the types of measurements that one plans to perform in TRADE, as well as an approach to the sequence of experiments. The main interest of TRADE, as compared to the MUSE experiments, is the ability of incorporating the feedback effects into the dynamics measurements in ADS and to address ADS operational, safety and licensing issues. The representativity of such experiments is also discussed.

II.2 Types of ADS experiments to be performed and their necessity

The types of the experiments that one needs to perform to validate different operational modes of a full power ADS fall into four broad categories. These are:

- start-up and shut down procedures,

- operation and monitoring of the system at steady state,
- monitoring of the time evolution of the reactivity, and
- practical coupling of an accelerator, a spallation target and the subcritical core.
- All four categories will be studied in TRADE, or discussed below.

Start-up and shut-down procedures for an ADS are subject to a number of discussions. The uses of the control rods or the change in accelerator power are two possible ways to pilot an ADS. Of course, one might envisage using a combination of both. In the experiments such as TRADE, one needs to cover all possible ways to operate ADS. One might want to use existing reactor start up procedures with the combination of the accelerator power increase protocols to deduce an appropriate way to start-up an ADS. In other words it is important to establish the relation between the increase in accelerator power and corresponding power raise of the core.

It is beyond the framework of this report to propose any sequence for the start-up or shut down; nevertheless one needs to foresee what kind of power transients must be studied to accommodate any of such sequences in the future for a full size ADS.

The first type of transient is an accelerator power transient. This kind of transients may be encountered during start up and shut down periods, and possibly as well during the change of the system power level. Accelerator-induced power transients are intimately related to the procedures that one uses to change the feeding power of the accelerator. It also covers the range of possible accelerator-related accidents and possible increase in accelerator power to compensate for the fuel burn-up at the end of the cycle. This kind of transient changes the power of the system and feedback effects have to be accounted for. Another important aspect of this kind of transient is the determination of the accelerator-reactor power relation. This is closely related to the study of the fluctuation of the reactor power as a function of accelerator power oscillations.

A second type is control rod induced transients. Along with a possible use of these to change system power level, they may be needed to make fine adjustments in reactor power oscillations due to uncertainties in the neutron production in the target. In ADS experiments in a thermal system such as TRIGA this type of transients can also be used to simulate burn up of the core. For the control of such transients one needs detailed information on the worth of the control rods. This worth will change as a function of the subcriticality level and flux distribution of the system.

The study of the operation and monitoring of the system is related to investigation of different core parameters during possible changes in system power. These include reactivity determination, source calibration, temperature and power profiles in the core, etc. In principle the transients associated with monitoring of the system are of the same nature as described above and represent less difficulty than, say, defining the necessity for the transients in start-up and shutdown regimes. Moreover, considering the surveillance, the follow-up of neutron production and the monitoring of the system from an engineering point of view , the TRADE project will be important for answering questions related to instrumentation (ex-core sensors,

in-core detectors: miniature fission chambers-nature of fissile deposit and geometry, location in the core and especially near the spallation target-Self Powered Neutron Sensors-expected life time of detectors…Fast and/or thermal on-line flux monitoring, fixed or mobile instrumentation ?….)

Monitoring of the time evolution of the reactivity. Equipment and methods to be used require particular attention. At steady state (or when characterizing the reference configuration) standard MSM (Modified Source Method) type techniques can be used to infer reactivity values. MSM is based on the fact that a detector response is inversely proportional to the reactivity, such that the ratio of counts (C) between two reactor states (ρ_1 and ρ_2) is:

$$\frac{C_1}{C_2} = \frac{\varepsilon_1 S_1}{\varepsilon_2 S_2} \frac{\rho_2}{\rho_1},$$

where S is the source strength and ε is the detector efficiency. However, in the use of MSM, care should be exerted, since the method does not discriminate between changes in counting rates due to changes in the intensity, and/or shape, of the neutron sources, or to changes in reactivity.

Moreover, during operation in real time one might not have time to numerically calculate correction constants and change in detectors' efficiencies required for the use of the MSM method. Therefore, one needs to explore a number of reactivity measuring methods based on the dynamics of the system. There are two different routes. First, one can examine the system response either to a flux perturbation or to the intrinsic neutron fluctuations, also referred as to the neutron noise. The time behavior is the same and is fully characterized either by the impulsion response in time domain or by the transfer function in frequency domain. The impulsion response is a sum of exponential functions of which the decay constants α_i are given by the in-hour equation. Two of these decay constants are noticeable, namely the prompt neutron decay constant α_p and the reciprocal α_T of the so-called "reactor period":

$$\alpha_p = \frac{\beta - \rho}{\Lambda} \text{ and } \alpha_T = \frac{\lambda \rho}{\rho - \beta}$$

assuming the one-delay-group kinetics and with the following notation:

- β the effective neutron delayed fraction,
- λ the delayed neutron precursor decay constant
- Λ the neutron generation time
- ρ the reactivity

It is noteworthy that α_p is the greatest decay constant while α_T is the least one. In frequency domain, the neutronic system acts as a low-pass filter with breakpoint pulsation α_p. The amplification of a perturbation always diverges at low frequency ($\omega << \alpha_T$) when the reactor is critical, it approaches a plateau in the middle frequencies ($\alpha_T << \omega << \alpha_p$), and drops off at the high frequencies ($\alpha_p < \omega$). For a subcritical system, the impulsion h(t)

response and transfer function H(ω) are as follows when considering the prompt neutron behavior as dominant (timescale of the order of $1/\alpha_p$):

TIME DOMAIN	FREQUENCY DOMAIN
$h(t) = e^{-\alpha_p t}$	$\left\|H(\omega)\right\| = \frac{1}{\sqrt{\omega^2 + \alpha_p^2}}$
Impulsion response	*Transfer function amplitude*

Although the kinetics parameters of TRADE ($\alpha_p = 70s^{-1}$ at critical) and a fast system such as MUSE ($\alpha_p = 6000s^{-1}$ at critical) are very different, the transfer functions relative to oscillating perturbations (source/reactivity) are identical except for a shifting to the lower frequencies for the slower TRADE (Ref. 2) response.

The flux perturbation approach can take advantage either of the exponential decrease or of the prompt jump. The one-group approximation for the point kinetic model predicts that the time dependence of the flux after a neutron pulse is injected is:

$$\frac{1}{\beta-\rho}\left(\beta e^{\alpha_T t} - \rho\beta e^{\alpha_p t}\right) \cong \frac{1}{\beta-\rho}\left(\beta - \rho\beta e^{\alpha_p t}\right), \quad \text{if} \quad -\rho \le \beta$$

The first exponential decreasing term driven by the delayed neutrons is negligible provided that ρ is less than 1 dollar. One can thus determine the slope α_p of the second exponential. The value of reactivity is then deduced from the definition of α_p assuming β/Λ as known and independent of the sub-criticality level. This method is referred as to the pulsed neutron-source (PNS) method in the literature. It is noteworthy that:

$$\alpha_p = \frac{\beta}{\Lambda}\left(1 - \frac{\rho}{\beta}\right), \quad \lim_{\rho \to 0} \alpha_p = \frac{\beta}{\Lambda} \quad \text{and} \quad \lim_{-\rho \to \beta} \alpha_p = \frac{\rho}{\Lambda}$$

One can thus estimate the sub-critical level ρ expressed in dollars provided that the ratio β/Λ is measured nearby critical.

The prompt jump Δn of the flux amplitude depends on the variation ΔS of the neutron source as follows:

$$\Delta n = \frac{\Delta S}{\beta - \rho}$$

assuming the delayed neutron source as constant. The reactivity value in dollars can then be obtained. The source variation can be provoked either by a harmonic perturbation [6] or a short break of the external source [7]. The well-known source jerk method using a Californium source is based on this rationale as well.

The noise approach is based on fluctuations of the neutron flux due to the fission-chain process of which the characteristic time is the reciprocal of the prompt neutron decay constant α_p. All these methods need to experimentally estimate a second-moment quantity:

- Rossi-α (RA): correlation function
- Noise transfer function: power spectral density (PSD)
- Feynman-α (FA): variance

The correlation function $C(\tau)$ of two neutron detector counts coming of the same fission chain and its Fourier transform the PSD function $G(\omega)$ are:

$$C(\tau) = \frac{D}{2F_0\alpha_p\Lambda^2} e^{-\alpha_p|\tau|} \quad \text{and} \quad G(\omega) = \frac{D}{F_0\Lambda^2}\left|H(\omega)\right|^2$$

with the Diven factor $D = \overline{\nu(\nu-1)}/\bar{\nu}^2$ and the fission rate F_0. Those two functions are here normalized by the number of counts Z of each detector. One can show that the variance of the number of counts is derived from the correlation function [8]. A well-known expression based on this variance is the Feynman formula also referred as to the variance-to-mean formula:

$$\frac{\overline{Z^2} - \bar{Z}^2}{\bar{Z}} = 1 + Y, \quad Y(t) = \frac{\varepsilon D}{\left(\alpha_p\Lambda\right)^2}\left(1 - \frac{1-e^{\alpha_p t}}{\alpha_p t}\right)$$

with the detector efficiency ε. That expression means that Z departs from the Poisson distribution because of correlated counts. Unlike the flux approach, the noise approach makes it possible to determine ρ, β and Λ not only through the time or frequency behavior of C(τ), G(ω) and Y(t) but also through their amplitude assuming D, F_0 or ε as known:

Method	Amplitude	Time/frequency behavior
RA	$\alpha_p\Lambda^2 = \beta\Lambda\left(1-\frac{\rho}{\beta}\right)$	$\alpha_p = \frac{\beta}{\Lambda}\left(1-\frac{\rho}{\beta}\right)$
PSD	$\left(\alpha_p\Lambda\right)^2 = \beta^2\left(1-\frac{\rho}{\beta}\right)^2$	
FA		

One can note that the amplitude of the PSD function, also referred as to the plateau is such that

$$\lim_{\rho\to 0}\left|H(\omega)\right| = \frac{\Lambda}{\beta} \quad \text{and} \quad \lim_{-\rho>>\beta}\left|H(\omega)\right| = \frac{\Lambda}{\rho}$$

Thus, with these two measurements, one can obtain a value of the reactivity in dollars.

However, the major drawback of all the noise methods is the long duration T that is required [9]:

$$T = 1/\delta t \left(e_N S_N \varepsilon\right)^2, \quad S_N = D/2\alpha_p \Lambda^2$$

with the neutronic noise source S_N, the expected relative error e_N and the time bin width δt. The duration T is longer for a thermal neutronic system as in TRADE than a fast one as in MUSE because of the much less important source noise S_N ($S_N \approx 3\times10^8$ s^{-1} in MUSE and $S_N \approx 6\times10^5$ s^{-1} in TRADE at critical). With δt = 10μs, $\varepsilon = 5\times10^{-5}$ and e_N = 5%, it yields a duration T of 12 hours or so.

As in the MUSE program [8], the noise techniques may be used to determine β and Λ in order to use them for estimating the reactivity ρ with the PNS method. The FA method may also be utilized using the data from several permanent detectors placed around the core.

The practical coupling of components will be achieved in the TRADE experiment. The engineering and operational issues related to the presence of a representative beam line, will be representative of generic problems of an ADS. In particular, the beam entrance in the core, the shielding issues both in the region above the core and around the bending magnets will be an important part of the demonstration of the concept. As far as the target, its cooling system and the coupling target-core will be extensively tested in a realistic configuration.

A recent theoretical work (Ref. 3) has pointed out the potential interest to conceive control type experiments to elucidate the coupling of the driver source and subcritical core. Work is underway to define these experiments.

Concerning the start-up, the first shot of the accelerator should be produced when the core is exclusively loaded with instrumented dummy elements (steel or depleted uranium-ZrH). This phase should be dedicated to the characterization of the target plus spallation neutron source residual spallation neutron source linked to beam losses along the beam pipe, etc. The information provided by the ancillary experiences can be precious in this phase, allowing having some reference points during the gradual loading of the core. Each successive configuration, in a reactivity scale, should be driven by the spallation source at very low power (continuous mode) and signals from multiple in-core and ex-core detectors should be recorded and analyzed before proceeding to the next loading configuration. When the core is sufficiently loaded with fuel elements (reactivity about 15,000 pcm negative), dynamic source techniques can be employed for reactivity measurements, in parallel with MSM techniques. These results should always be analyzed in the context of the earlier pre-startup measurements. Then, when the results become interpretable in terms of coherence about the subcritical level, it is possible to analyze the system response at different accelerator powers, source importance, etc. At this stage it's also possible to start to verify some system basic neutronic parameters, like control rod worths, temperature coefficients etc. This will go on, till the first reference subcritical configuration is loaded.

The experiments previously described will be very important for the validation of operating methods for a future ADS, and they can only be performed in a facility that has reactivity feedback effects at power.

Normally, withdrawing enough control rod(s) to generate a reasonable stable positive period (perhaps 30 seconds or so) starts a TRIGA reactor. When feedback appears at about 1 kW, the operator must then continually withdraw control rods or there will be no increase in power. There is also an effect from xenon and samarium poisoning as the reactor is operated continuously. Thus, the TRIGA core loading must have enough excess reactivity to overcome both the feedback coefficient and the poison effect. This excess reactivity has to be available in the control rods to hold down the reactivity to about 0.96 (for example) when the reactor is cold, but have to be withdrawn at power to compensate for the power coefficient (up to 3000 pcm at 1 MW) and poison effects (up to 1900 pcm at 1 MW) in order to maintain k=0.96. The startup of any reactor system, sub-critical or not, requires continuous monitoring of the neutron flux level and knowledge of the reactivity before startup is initiated. Thus, the startup will likely begin with the accelerator at a relatively low current to ensure neutron flux monitoring. Following that, there will likely be an alternating sequence of increase in current and withdrawal of control rods. Note that in the example of a target operating reactivity of k=0.96 but with up to 5000 pcm carried in the poison and feedback, one cannot simply turn off the accelerator to shut the system down. If this is done, as the reactor power decreases due to loss of source, the reactor could end up in a supercritical state as the feedback reactivity decreases (of course feedback will again come into play, and the reactor will seek some steady power). Thus, as in a conventional reactor, it appears that a scramming of the control rods must initiate the shutdown, followed by shutdown of the accelerator.

As we have seen above, the dynamics of an ADS must be explored across its full range of operation. With an ADS the transient behavior in “source dominated” deeply subcritical configurations will be very different from “core dominated” behavior in configurations near criticality (as quantified by the core delayed neutron fraction) when the standard feedback effects are dominant.

For this reason, experimental investigations must be performed over a wide range of core powers and subcriticalities. Specifically, there is a strong need to experimentally validate theoretical models in the cases where (1) core dynamics regulates the system’s response to external perturbations, (2) core power levels are high enough for core dynamics feedback to be important, and (3) external source behavior determines the core dynamics behavior.

This type of behaviour and the transition between the source dominated and the core dominated modes, that can happen in the same core during the irradiation cycle due to burn-up reactivity swing, should be carefully investigated, in order to develop appropriate monitoring and control systems for the power distribution in the core, but also in order to choose appropriate reference subcriticality levels.

Although MUSE experiments can provide the validation of the basic physics needed for ADS qualification, there are nevertheless important elements missing. For example, a zero power assembly cannot investigate the relationship among source importance, current, power and reactivity. For this, some heat rejection capability is needed that is not found in zero power critical facilities. In the same vein, the dynamic behavior of feedback effects induced by power and temperature cannot be studied at zero power.

Present design and parameter studies of ADS for transmutation indicate that a wide range of subcriticality regimes has to be envisaged. In fact most of designs require a subcriticality

ranging from $K \simeq 0.94 - 0.95$ to $K \simeq 0.99 - 0.995$. In the "low" or "high" K range, the dynamic behaviour of the ADS may be very different. As far as representativity, despite the fact that the proposed experiments are made in a thermal neutron spectrum environment and the preferred configurations of ADS for transmutation are related to fast neutron spectra, the delayed part of the kinetic response to any perturbation is similar in thermal spectrum reactors (with $\beta \simeq 0.007$ and $T \simeq \sim 10^{-4}$ sec) or in fast spectrum reactors ($\beta \simeq 0.002 \div 0.003$, $T \simeq 0.5 \times 10^{-6}$ sec).

As far as reactivity monitoring and control, besides the safety and control rods, the design of which is often complex and inducing high level of uncertainties, a specific absorber can be prepared to replace a standard fuel rod. In such a way, a reference perturbation is established, the uncertainty of which is proved before the experiment and verified during the program.

The design of this absorber (a priori with ^{10}B) can be such that the neutronic absorption is equivalent to the standard fuel rod absorption. With this precaution, the uncertainty on the perturbation effect due to the substitution is reduced. The chemical composition of this absorber can be carefully checked and a neutron efficiency test performed in a suitable thermal reactor. With only one absorber, the range of subcriticalities which can be explored, can vary by a factor 4 (supposing a factor 2 for the direct and adjoint flux, between the center of the core and its periphery).

In the same way, a reactivity controlled fluctuation system can be envisaged to be able to create a controlled power fluctuation for the subcritical system. This system and the associated detection of the power fluctuation can be designed to respond starting at a subcriticality level (for example -500 pcm), which can be adjusted.

As far as the coupling of the target and the subcritical core, the TRADE experiment will bring interesting elements to understanding the dynamic behavior of an ADS. For example, in the case of source shutdown, after less then 1 μs most of the spallation neutrons (~99 %) will be absorbed. Most of the prompt neutrons in the core will disappear too, according to the period $\Lambda/(\rho - \beta)$ (i.e. few μs in a fast neutron system of few ms in a thermal neutron system, depending on the subcriticality level).

Then, there will be a power decrease from initial power level p_0 down to a level p_1 determined essentially by delayed neutrons $p_1 = p_0/(\frac{|\rho|}{\beta} + 1)$. This takes place both in thermal and fast systems. The p_1 level will be more or less relevant as compared to the decay heat and will also depend on subcriticality level.

This behavior will be easily explored with the TRADE experiment at several levels of subcriticality. The effect of feedback will also be representative since temperature variations have a characteristic time much longer than a millisecond range quoted above, the last covers both thermal and fast neutron cores dynamics.

II.3 Beam trips

The dynamic behavior of the system in response to unavoidable beam trips (despite the requirement expressed for the TRADE accelerator) will be explored experimentally in the TRADE experiment in a significant manner.

Short beam trips (less than 0.1-1 s) have been shown not to be a major concern for the safe behavior of the system. Beam trips with duration longer than a few seconds have to be investigated experimentally with detectors sensitive to temperature and neutron population variations at different spatial points in the core and close to the target. In fact, modifications of the neutron flux distributions are expected after source shutdown, according to the time/space variation of the spallation neutron, prompt neutron and delayed neutron contribution.

II.4 Representativity of the experiment

With respect to dynamic behaviour trends, interesting results have been obtained, which show that the effect of the TRIGA feed back coefficients is such that they exhibit with significantly different amplitude, varying with the subcriticality of the core (see Figure 1, Figure **2**, and Figure **3**). The power increase for reactivity insertions of 50 and 10 cents respectively, in 2 seconds, is shown at three different values of subcriticality. Experiments can then be envisaged to verify experimentally the dynamic response of the core, together with the experimental determination of the relative subcriticality level.

Similar effects have been explored in a sodium-cooled ADS (Figure 4, Figure 5, Figure 6).

At deep subcritical configurations the system's response is dominated by the source behavior. After a prompt neutron jump, reactor power stabilizes at a certain level. Once the system is close to the criticality, the 'core dominated regime' become more important: depending on the magnitude of feedback, the reactor either 'runs away' or once again stabilizes at certain power level. Such situations are closely connected with the question of a proper level of subcriticality for a steady operation of an ADS. The similarity of Figures 1-3 with Figures 4-6 is an illustration that a thermal system can be efficiently used to study the dynamics of an ADS. The calculation for the transients in a Na cooled ADS were performed with three types of feedback typical for a fast reactor:

Radial core expansion:	1.6×10^{-3} \$/K,
Core coolant void worth:	-3\$,
Fuel Doppler (T dk/dT):	-0.0005.

The considerations noted above make it clear that there is much to study regarding the startup and shutdown of an ADS. The TRIGA is ideally suited to these studies because it has feedback reactivity, and is influenced by the buildup of fission product poisons. The inherent safety of the TRIGA makes it possible to explore regimes close to critical, or even super-critical.

A particular feature of the TRADE experiment is related to the large prompt temperature coefficient of the TRIGA reactor. This feature allows in TRADE transients which are

induced by relatively limited source variations and which can be used to explore important source variation transients in a reference ADS of higher power.

The external neutron source for the TRADE experiment is a spallation source. Tungsten is chosen for the target material. High-energy protons (100 MeV or so) are provided by a cyclotron situated in a building separated from the reactor. The beam line in TRADE is representative of the one that might be used in a 'real size ADS'. After several bendings the beam enters the core vertically from above. The accident scenario that one can foresee in such a geometry is a loss of magnet deflecting capabilities and following defocusing of the beam. High-energy neutrons produced in spallation reactions might induce significant damage in surrounding structural materials and neighboring fuel assemblies. Therefore, one must carefully study the spectrum and intensity of the resulting neutron flux to address issues related to shielding. Also in situations related to the defocusing of the beam, one must also assure that all necessary measures are taken to prevent irradiation of the structural materials and staff.

In order to give a comprehensive answer to the question of representativity of the experiment, the impact of the different proton energies (100-200 MeV in TRADE vs. 0.6-1 GeV in an ADS) on the kinetic behaviour should be also evaluated, taking into account the characteristics of the subcritical configurations (thermal neutrons in TRIGA and very probably fast neutrons in a transmuter ADS). In principle, this evaluation can be done by comparing time dependent Monte Carlo simulations relevant to a beam trip in a prototypic system at full power and in a TRADE configuration having the same subcriticality level (about –8$). The choice of the beam trip case has two motivations: the general interest in unexpected beam trip behaviour itself and the interest in source jerk type measurements. Monte Carlo tallies to be compared are relevant either to detector responses in particular system positions or to the total flux behaviour. In both cases, tallies to be compared can be normalised to their initial values (just before the beam trip).

It is well known that one of the expected differences between the couples of normalized responses is due to the different prompt neutron lifetimes in the two systems (thermal vs. fast). This difference can be roughly evaluated using point kinetics. It is expected that this difference should not preclude the possibility of using (either in TRADE or in a prototypic system) source jerk type measurements to evaluate a system "subcriticality level". Moreover, this same difference has not a significant impact on any coolant temperature drop (in fuel, coolant, etc.) because, due to the heat transfer processes, temperature variations have a characteristic time (about 1 s) that is much larger than the prompt neutron lifetime.

A second difference between the couples of normalised responses is in principle due to the different amplitude, shape and time behaviour of the neutron source generated by the hard component of spallation that appears below 20 MeV after downscattering, (n,xn), etc. In principle, this can only be investigated by a direct comparison of the Monte Carlo calculations in the two different systems. Both the Monte Carlo calculations should involve time dependent simulations, including protons, spallation, and a full energy range neutron calculation. However, the time to "slow down" the high energy neutrons (also by (n,xn) process) should be of the same order of magnitude of the neutron lifetime in the system, and not less then 85% of spallation neutrons should appear directly below 20 MeV; the difference among the phenomena above 20 MeV can likely also be neglected in many practical cases (e.g., to evaluate any possible temperature variation in the systems).

A first answer to the representativity problems identified above can be obtained by calculations (and possibly validated by experiments):

- Preliminary determination of the average time needed for a source neutron emitted with an energy above 20 MeV to produce neutrons with energies below 20 MeV; this evaluation requires Monte Carlo static calculations;

- Comparison of the results produced by different Monte Carlo simulations relevant to the same system (either the prototypic system or a TRADE configuration). In particular, results obtained by a complete Monte Carlo simulation should be compared to the results obtained by an approximate Monte Carlo simulation, carried out under hypotheses similar to those generally assumed in deterministic calculations: i.e. that the system is driven by the neutron volume-source below 20 MeV only. The volume-source below 20 MeV should be calculated once for all before the beam trip by means of a complete Monte Carlo and should be "frozen" to be considered constant in energy and shape during the transient of the approximate calculation.

In parallel with a numerical approach, it is possible to conceive also an analytical approach that isolates the role of the phenomenon mentioned above. In particular, in the case of idealised paradigmatic configurations for which solutions can be given in a closed form, it is possible to study in a parametric way, changing a time delay parameter, the effect of such physical phenomenon for transient situations. In such a way, by the independent evaluation (by Monte Carlo estimates, as above described) of the order of magnitude of the average energy-transit time from energies above 20 MeV to energies below 20 MeV, it is possible to study the influence of the effect and its relevance on the kinetic response of the system.

Preliminary results have been obtained, related to the effect of the buffer material surrounding the target, the type of the core (fast versus TRIGA), and the energy of the incoming protons (100-200 MeV in TRADE vs. 0.6-1 GeV in an ADS) on the kinetic behavior. The MCNPX code was used with a simplified model of the TRIGA reactor: an empty ring B (filled either with water or led-bismuth eutectic) with the following rings of fuel elements replaced with an annular layer. The purpose is to evaluate the time dependence of the neutron population in the fuel zone after the external neutron source is turned off. The time dependence of the neutron population was studied with the following parameters:

(1) two energies of proton beam: 110 and 1000 MeV;
(2) two materials filling the B ring: water or led-bismuth eutectic;
(3) two fuel types: typical TRIGA fuel and a fast reactor fuel.

The results are shown in Figure 7 and Figure 8. The time scale refers to the moment of beam shut-down. At longer times (of the order of 10^{-5} s and longer) the results of our calculations yielded statistical errors of more then 10%. Therefore in this time range the results should only be considered as the demonstration of general trends. The results of Figure 7 are obtained having "turned off" the fission process, to allow a comparison between thermal and fast neutron systems as far as the effect of spallation neutrons only. The results of Figure 8 are related to the total (i.e. both spallation and fission neutrons) or spallation neutron flux. The results allow then to compare the neutron population time evolution with and without fission.

It was concluded that in the typical thermal TRIGA fuel the neutron population (both spallation and total) in the core is not a function of the material filling the ring B: the results for the water and LBE are both close for 110 and 1000 MeV. Therefore, Figure 8 shows only results for the water filled ring B case.

For the same material (water or LBE) in the ring B, the results for different proton energies are very close. Nevertheless, neutrons born from 1 GeV protons disappear faster than those born from 110 MeV. However, the choice of the beam energy is not related to the neutronics of the core, but only by required reactor power and technology of the beam-target coupling. A Monte Carlo simulation showed that the faster disappearance of neutrons born from more energetic protons can not be fully explained by the higher probability for neutrons in this case to escape in the direction of the beam. The faster disappearance is noticeable at longer times after the beam is turned off, where the statistical errors are high and can be related to the poor statistics.

The time dependence of the spallation neutron population was also verified as a function of the fuel type. In the fast reactor fuel in microseconds range, spallation neutrons disappear approximately two times faster than in TRIGA fuel. This is due to the higher leakage from a fast core (bigger mean free path) and higher cross section of the TRIGA fuel as compared to the fast reactor fuel. Since in both cases spallation neutrons disappear in microseconds, the reactivity measurement techniques, which will be validated in TRADE, will apply to a 'real' ADS with fast spectrum.

It is worth mentioning that in all cases, a few microseconds (~6-10 microseconds, depending on the case) after the source is turned off, the spallation neutron population is reduced to at best 5 % of its initial value. As to the fraction of high-energy spallation neutrons (above 20 MeV), they completely disappear after ~2 microseconds.

II.5 Experiments in the subcritical core and relation with the MUSE experiments

As indicated above, the future operation of an ADS at reference power (eg, 100 MWth) requires an experimental program to validate the ability to calculate parameters important to safety (e.g., β_{eff}, fission rates) and the ability to monitor operating parameters (e.g., power to current ratio, levels of sub-criticality, effect of feedbacks). The requirements for validation of safety and operational parameters lead to the types of experiments that must be performed:

- Source importance
- Flux distributions and basic reactor parameters
- Reactivity measurements
- Proton current/power relations

Importance of the source neutrons is one of the important characteristics to be studied for several reasons. On one hand, one might consider to operate the ADS by a change in the source importance, in other words by adjusting buffer material to the power requirements. On the other hand, such measurements are important because of their influence on the accuracy and validation of the reactivity monitoring of the system.

One must also measure the parameter φ^*, ratio of the importance of source neutrons to fission neutrons:

$$\varphi^* = \frac{\langle \Phi, S \rangle / \langle S \rangle}{\langle \Phi^*, M\Phi \rangle / \langle M\Phi \rangle}.$$

In the last formula triangular brackets mean the integration over the region of interest $d\vec{r}$ and the energy interval. The source importance is related to the accelerator current i as follows:

$$i \approx P \frac{1}{\varphi^*} \frac{\nu}{Y} \left(\frac{1 - K_{eff}}{K_{eff}} \right)$$

with the following notation: P-reactor power, ν-number of prompt neutrons, and Y-yield of spallation neutrons per proton. Thus, for given power and subcriticality, the higher source importance, the lower electron current required for the accelerator. The importance can be deduced from the measurements of fission rates in the core. In a similar manner, the relation of the accelerator power and core power in presence of feedback can be investigated. This can be done only in a system with sufficient power levels and substantial feedback.

Another aspect of the source deals with the behavior of high-energy neutrons. This is important for the material damage, power distribution in the system and efficiency of different reactivity measurements. The last point should be considered separately, since the presence of high-energy neutrons and a buffer might significantly change neutrons' lifetime. Consequently, this will produce a delay in detector's registration, degrading therefore the accuracy of, for instance, NPM (Neutron Pulse Method).

Finally we mention the measurement of radial and axial power distribution in the core by means of micro-fission chambers placed at several points in the core. Spectral information can be deduced from U238 and Np237 fission rates. This information is important for the study of behavior of different buffers and possible induced damage in structural materials.

Studies of the effects of core de-coupling, validation of calculations of fission rates and β_{eff}, and techniques of reactivity measurement will be performed in the zero power MUSE experiments. However as mentioned above, it will not be possible to study operational aspects of an ADS such as power/current relations, startup and shutdown scenarios, and the effects of feedback at operating power in MUSE. This will require a prototypical spallation source coupled with a sub-critical medium that is capable of operating at a power at which feedback dominates the kinetic behavior. The experiments in a TRIGA reactor described here are designed to bridge the gap from MUSE to an operating ADS. At the same time, methods developed in the MUSE program will be validated in the TRADE experiments, thus demonstrating a sort of `generic validation' of methods developed in a fast system applied to a thermal system. We have proposed that the phase I experiments would measure the source importance from Cf, DD, and DT. Thus, the lower energy regimes of source importance are investigated in the first phase. In total, TRADE will contribute source importance

measurements for a fission source, DD source at 2.5 MeV, DT at 14 MeV, and spallation at hundreds of MeV. We can view the validation process leading to an ADS as:

CONFIGURATION	SOURCE	KINETICS	POWER EFFECTS
MUSE	DD/DT	FAST	NO
TRIGA	DD/DT	THERMAL	NO
TRIGA	SPALLATION	THERMAL	NO
TRIGA	SPALLATION	THERMAL	YES
ADS	SPALLATION	FAST	YES

With the middlethree stages demonstrated in TRADE. As we can see from this table, we approach the validation to the ADS by not changing more than one parameter from one configuration to the next.

II.6 Reference subcritical core for TRADE

As in the MUSE program, a preliminary step will be measurements taken at a reference configuration which is at critical or just subcritical (50-100 pcm negative). This reference must be reasonably close to the first subcritical configuration envisaged with the accelerator (i.e., without B ring fuel). In addition, even though the accelerator has not been installed at this point, there should be some materials/structures in the core that simulate the beam tube and target. The approach to criticality in this configuration is performed in the standard way with the aid of the Am-Be startup source (which is normally placed in the periphery of the core, but for this experiment it will be placed in the centre in order to assess the source importance).

At criticality, basic measurements will be performed, such as control rod calibration, fuel temperatures, temperature coefficient measurement (obtained by step insertions of small reactivities while at power), delayed neutron fraction, and prompt neutron generation time. At this time as well, the fission reaction rate, source importance, and spectral index measurements should be performed (as in MUSE), because of interest in the deviation (from the reference) of these quantities under the influence of the source when the accelerator is finally coupled. Once basic core neutronic parameters at the reference configuration have been determined, one can define the first core configuration to be coupled with the accelerator. Different core configurations at intermediate subcriticality levels, obtained by fuel element movements and/or control rod adjustments can be analyzed.

II.7 Experiments with DD and DT source

As the next step, it will be beneficial to perform experiments with a DD and DT source before the spallation source is assembled. This will provide a much smoother transition from MUSE to TRADE as explained later in this report. We will obtain source importance for Am-Be, Cf, DD, DT, and spallation neutrons in the same configuration. Because of the great uncertainties in cross-sections above 20 MeV, this step is almost essential to understanding the results at the higher energies. The lower energy source importance results serve essentially as a kind of calibration factors. On the other hand, the (d,T) source operating in

pulsed mode should allow investigating the feasibility to monitor the subcriticality level for TRADE (at least at zero power) by pulsed neutron source techniques. In addition, measurements with a central source can give indications about the best detector locations in the core. Another benefit of this step is it will allow all the data acquisition equipment and analysis techniques to be tested.

II.8 Conclusions

The TRADE experiment represents a necessary step in the process of validation of the ADS concept, the next step being the demonstration of waste transmutation in a prototypical ADS.

The representativity of the experiment has been discussed. The impact of having a thermal neutron spectrum and an external source due to relatively low energy (100 MeV) protons, is not significant in terms of the overall validation of the dynamic behaviour of an ADS in different regimes ("source" – dominated, "core feedback" – dominated), of the start-up and shut-down procedures, of the monitoring of reactivity variation during irradiation etc. Moreover, the "full scale" demonstration of the coupling of the real components (accelerator, target, subcritical core) will bring invaluable elements to future ADS engineering designs.

The TRADE experiment should then provide a short-term demonstration of relevant elements of the ADS concept. The successive campaign of experiments in TRADE should consolidate and enlarge the experimental validation data base.

III. TRIGA core physics with deterministic method

III.1 Core description

The TRIGA core (Figure 9) consists of a cylindrical structure immersed in water, which serves as primary coolant. The core is arranged in an array forming an annulus with seven coaxial cylindrical rings of fuel elements including the central ring. These rings are named by letters from A (central) to G, the outermost ring. The numbering system starts with B-1 in the same azimuthal position as the regulating (REG) rod in the F-ring, and the numbering order in each ring is clockwise. The core, which is surrounded by the graphite reflector, consists of a lattice of fuel elements, graphite dummy elements, control and regulation rods. There are 127 locations divided in seven concentric rings (from 1 to 36 channels per ring). The locations are loaded with the different components depending on the power level required. These locations are contained within top and bottom aluminum grid plates: 126 holes for fuel elements, control rods, dummy graphite and a central thimble for high flux irradiation. One channel houses the Am-Be source, while two fixed locations (the central one and a peripheral) are available for irradiation or other experiments. The diameter of the core is about 56.5 cm while the height is 72 cm. Neutron reflection is provided by graphite contained in an aluminum container, which is surrounded by 5 cm of lead acting as a thermal shield. An empty aluminum tube (15 cm diameter and 0.6 cm thick) traverses the graphite reflector tangentially to the reactor core for thermal flux irradiations. The reactor and the experimental facilities are surrounded by a concrete shield structure. The core and reflector assemblies are located at the bottom of an aluminum tank (190.5 cm diameter). The overall height of the tank is about 7 m therefore the core is shielded by about 6 m of water. The fuel elements

consist of a stainless steel clad characterized by an external diameter of 3.73 cm and a total height of 72 cm end cap included (Figure 10).

The fuel is a cylinder (38.1 cm high, 3.63 cm in diameter, 5.9 g/cm3 of density) of a ternary alloy uranium-zirconium-hydrogen (H-to-Zr atom ratio is 1.7 to 1; the uranium, enriched to 20 % in 235U, makes up 8.5% of the mixture by weight: the total uranium content of a rod is 190.4 g, of which 37.7 g is fissile) with a metallic zirconium rod inside (38.1 cm high 0.5 cm in diameter, 6.49 g/cm^3 of density). There are two graphite cylinders (8.7 cm high, 3.63 cm in diameter, 2.25 g/cm^3 of density) at the top and bottom of the fuel rod. Externally two end-fittings are present in order to allow the remote movements and the correct locking to the grid. The regulation rod has the same morphological aspect as the fuel rod the only difference is that instead of the mixture of the ternary alloy uranium-zirconium-hydrogen there is an absorber (graphite with powdered boron carbide); the inner Zr cylinder is not present. The control rods (Figure 11) are "fuel followed": the geometry is similar to that of the regulation rod with the bottom graphite cylinder replaced with fuel. The graphite dummies are similar to the regulation rod but without boron inside the central volume.

III.2 DIF3D model of the core with cross section calculated with WIMS-ANL code

In this paragraph we describe a calculation of the TRIGA reactor with the aid of the diffusion theory DIF3D code. Hexagonal-Z geometry with nodal option for the full reactor core is used. We refer the reader to the Ref. 4, 5 and 6 for the description of the reactor geometry and compositions. The pitch (d) of the hexagons to be used in this model was calculated based on the 'equivalence model". In Ref. 5 the equivalence to preserve the coolant (water amount) up to row F of the core was used; the result is d=4.365 cm. A calculation using the whole core radius (beyond ring F) yielded d=4.504 cm. To be consistent with the Ref. 5 for now we fixed our pitch at d=4.365 cm.

A detailed hexagonal TRIGA geometry was used in our calculation. When constructing the geometry input the following assumptions were made:

1. The void in the Loop pin was smeared in the density of the structure materials since diffusion theory cannot handle a void region and the peripheral position of the pin suggests that its influence on the core reactivity should not be significant;
2. The void in the Source pin was smeared in the density of aluminum for the same reasons;
3. The void in the Rabbit pin was smeared in the density of the structure materials for the same reasons.

The control and regulation rods were modeled as described in the nominal TRIGA configuration corresponding to the Ref. 4.

For the cross section calculation we used the WIMS-ANL code to generate group cross sections for different compositions of the reactor fuel pins, control rods and special assemblies in the axial direction. As a first step a 9 group energy structure was chosen with the following energy boundaries: 1e-5, 8.E-02, 1.8E-01, 6.25E-01, 1.3, 4, 1.48730E+02, 9.118E+03, 5.E+05, 1.E+07 eV.

We do not list here all the axial geometry cuts of the TRIGA's assemblies to calculate cross sections, but instead list the following major ones for a fuel hexagonal assembly:

1. The water section (under and above TRIGA pins);

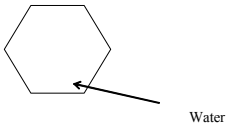

2. Graphite section

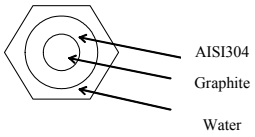

3. Fuel section

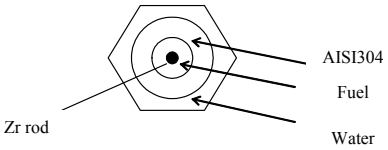

4. Grid section

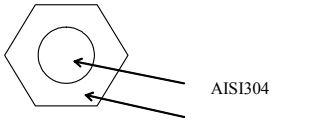

5. Absorber section (for the Control and Regulation rods)

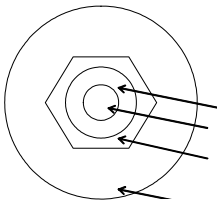

Ring of fuel section material simulating 6 surrounding fuel hexagons with number densities taken from the corresponding WIMS calculation for fuel section in 3

The other cuts include all parts of special assemblies such as loop, rabbit, source, graphite and lead assemblies. The information on the exact partition of these assemblies in the axial direction to calculate cross sections is available upon request. We used he combination of the resulting cross sections in other parts of the reactor as needed.

All seven rows (A to F) of the TRIGA core were modeled in DIF3D code with hexagons with appropriate axial partition in the same way as it was modeled in Ref. 5. The actual reflector and water tank, which is 52.92 cm cylindrical layer containing graphite at certain positions, was modeled by 12 rows of hexagons (pitch d=4.365). To preserve the total actual amount of water, we adjusted the density of water in the whole reflector, taking into account the void in the tangential and radial channels. Also, an 'average' for all elements fuel composition (Ref. 4 and 5) was used in the calculation of the cross sections with the WIMS-ANL code. In the following discussion the model described above is called *model 1* (Figure 12). All fuel assemblies are described with the same density ρ=5.920345 g/cm^3 and composition given as follows:

Weight isotopic fractions:

U235	0.0137233
U235	0.0640722
Natural Zr	0.9056940
H	0.0165104.

To check our results we constructed an MCNP deck using the exact same geometry (hexagonal modeling for the core and reflector) as for the DIF3D. Once again, an average fuel composition was used. In the following this model is called *model 2* (Figure 12). The difference between models 1 and 2 is: 1) calculation method, and 2) model 1 uses homogenized cross sections as calculated by WIMS.

Previously, an MCNP calculation in mixed hexagonal-real geometry was carried out (Ref. 5). In this calculation the core itself was modeled with hexagons, and the reflector and water tank were left intact (not replaced with hexagons, but represented by cylindrical layers). The deficiency of this model is that seven rows of the core's hexagons cannot be fitted into the core vessel radius. Therefore, supplementary fractions of water filled hexagons were added. Also, one fuel assembly and 5 graphite and special assemblies got 'cut' by this geometry (did not appear in its initial shape). The material concentrations for the fuel assembly were adjusted to conserve the mass. In this case the authors used the detailed fuel compositions that differ from element to element. In the following discussion this model is denoted *model 3*.

Finally, the reference MCNP model with actual geometry (both for the core and the reflector) is called *model 4*. This model also uses the detailed fuel composition description.

III.3 Results

III.3.1 Bare core

In order to check the coherence of the cross sections for the TRIGA core's compositions we first studied the configurations without any reflector. The extrapolated flux zero boundary condition was used for the diffusion calculations. The following table summarizes our results for two different core configurations: 1) UPP-all control rods are withdrawn; 2)

NOM-control rods are partially inserted to reach the 'nominal' TRIGA configuration number 235.

Model Config.	DIF3D (diffusion) hexagonal *Model 1*	DIF3D (transport) hexagonal *Model 1*	MCNP hexagonal *Model 2*	Error *Model 2* vs. *Model 1 (diffusion)*	Error *Model 2* vs. *Model 1 (transport)*
UPP	1.00375	1.01311	$1.00789 \pm 0.15\%$	Δk=0.413; $\Delta\rho$=408 pcm	Δk=-0.522; $\Delta\rho$=-511 pcm
NOM	0.95451	0.96243	$0.96235 \pm 0.15\%$	Δk=0.738; $\Delta\rho$=803 pcm	Δk=0.080; $\Delta\rho$=9 pcm

Table 1 Bare core results

It is seen that the agreement between all studied models/calculation techniques is fairly good.

III.3.2 Complete reactor configuration

We study here the complete geometry of the TRIGA reactor that includes the reflector. The adjustment of the materials densities in the reflector and the influence of the method of adjustment are analyzed in this section. Neutronics of the core suggests that the adjustment using 'layer by layer' method, starting from the closest to the core materials, is appropriate. The second option is to adjust the total amount of all materials in the reflector and use the resulting densities in any reflector positions. The difficulty rises from the impossibility to represent the void in the tangential and radial channels in the diffusion theory codes and the approximate nature of the replacement of the real geometry by hexagon layers. The void was taken into account in the adjusted densities. Appropriate hexagon geometry was used to represent the layers of water, graphite and lead in the reflector.

First, we used "layer by layer" approach. In this case one derives the following adjustments to be in order:

1) First two graphite layers. The adjustment factor for densities is $\rho_{new} = 1.0086\ \rho_{old}$;
2) Next 3 graphite layers. The adjustment factor for densities is $\rho_{new} = 1.3475\ \rho_{old}$;
3) The lead/graphite layer. The adjustment factor for densities is $\rho_{new} = 1.4127\ \rho_{old}$;
4) The water in all layers. The adjustment factor for densities is $\rho_{new} = 1.1882\ \rho_{old}$.

As an example, we report here results for the core configuration in which the control rods were in 'UPP' position. The following table represents the results.

Model Config.	DIF3D (diffusion) hexagonal *Model 1*	MCNP hexagonal *Model 2*	MCNP (mixed) *Model 3*	MCNP (real) *Model 4*
UPP	1.081717	$1.07976 \pm 0.14\%$	$1.05571 \pm 0.10\%$	$1.05463 \pm 0.12\%$

Table 2 Complete reactor configuration results

Using this approach, the MCNP hexagonal model (*model 2*) gives overestimated result as compared to the MCNP calculation in mixed (*model 3,* Ref. 5) and real (*model 4,* Ref. 5) geometries. However, the corresponding DIF3D results for the diffusion (*model 1*) are reasonably close to the MCNP hexagonal model. This is expected since a) it was previously proven that there is no significant impact produced by the homogenization procedure in WIMS-ANL (see bare core results, Table 1), and b) there is a complete correspondence of the geometry of the system in both cases. Although, it is seen that the DIF3D result and the MCNP hexagonal *model 2* results are coherent, they differ significantly from the MCNP real and mixed geometry results. The adjustment of water by 'layer by layer' technique (as described above for graphite) did not significantly affect the results of the calculations. Therefore, one concludes that there exists a geometry/homogenization affect in the reflector that amounts for the ~2400 pcm of error. This effect must be mostly attributed to the absence of the reflector cover in the DIF3D calculation (*model 1*, due to the impossibility to model it), local channels void effects (for the same reasons), as well as to the impossibility to explicitely represent the reflector's components by hexagon layers. We also mention that the results for *models 3* and *4* were based on the detailed fuel compositions (see Ref. 4 and 5) and models 1 and 2 are based on average fuel composition. Our estimation show that this effect accounts for ~ 400-600 pcm (depending on the reactor configuration) to decrease the k_{eff} of the models 1 and 2.

To understand how the impossibility to model certain components of the reflector affects the calculation, we introduced some modifications in the *model 3*. In this model we eliminated the unwanted fractions of water in the core, the channels in the reflector, and the reflector cover, replacing them with void and graphite correspondingly. The resulting $k_{eff}=1.06995 \pm 0.15\%$ is much closer to the values obtained with DIF3D and MCNP hexagonal models. To further prove that the difference in results comes from the absence of exact geometry parity, we moved the reflector in *model 3* closer to the core by the distance equal to the reflector cover thickness (as it is the case in the hexagonal models). This pushes the graphite closer to the core and should increase the reflection of neutrons. The result is $k_{eff}=1.07163 \pm 0.15\%$, which is within 800 pcm with the hexagonal *models 1* and *2*.

To further confirm the noted trends a modified version of *model 2* was explored. We modeled the reflector cover, tangential and radial channels, and the reflector cover in hexagonal geometry with MCNP. The axial cut at the level of the tangential channel is shown in Figure 13. The total amount of water in the reflector was adjusted to the real geometry model (*model 4*) $\rho_{new} = 1.1882\ \rho_{old}$. The density of the first graphite layer requires a small adjustment $\rho_{new} = 0.9160\ \rho_{old}$. The rest of the graphite was adjusted correspondingly $\rho_{new} = 1.3237\ \rho_{old}$. The reason to adjust the first layer of graphite separately is based on the fact that the reactor's multiplication factor is very sensitive to material at the core's proximity. The result of the MCNP hexagonal model calculation that takes into account local void and reflector cover effects is $k_{eff}=1.05316 \pm 0.13\%$. This is in very good agreement with *models 3* and *4*.

To remedy the deficiency of the hexagonal model in DIF3D identified above, we have two possible approachs: 1) try to model void channels in DIF3D and 2) adjust reflector densities. The use of the first option is a delicate procedure. On one hand it is possible to envisage introducing low-density, low neutron cross section material in certain assemblies to model

the channels (O^{16} in our calculation). On the other hand this will result in poor convergence of the calculation. We introduced the tangential channel in the DIF3D calculation with the following adjustments: the reflector cover was taken into account in the density of the first hexagon layer. The rest of the materials' amount was conserved separately. In this case we could only reach convergence with a O^{16} density of 0.005 a/cm-barn with the precision of 0.001 on the multiplication factor. The result is k_{eff}=1.07281. This is an improvement as compared to the previous result, but the value of approximations and precision used in such a calculation is difficult to quantify.

The second approach is straightforward. We performed a sensitivity study and concluded that the density of water adjusted in both ways (total amount or 'layer by layer') does not significantly affect the results of calculations. The same conclusion can be derived for the lead density (to conserve the total amount of lead the appropriate density change is $\rho_{new} = 1.2881\ \rho_{old}$). However, the k_{eff} was found to be very sensitive to the density of graphite (as was also mentioned above).

We judge in this case that the total amount of water and lead should be preserved and one should reach the coherence of results between real and hexagonal geometry through the adjustment of the graphite density. The graphite density needed to be lowered from ~0.13 a/cm barn to ~ 0.07 a/cm barn to match the results of the MCNP hexagonal and DIF3D models. Of course, this adjustment is arbitrary and not final, more experimental evidence is necessary to derive the appropriate graphite density . In summary, the following density changes are in order:

1) Water density adjustment $\rho_{new} = 1.1882\ \rho_{old}$ (the total amount is conserved);
2) Lead density adjustment $\rho_{new} = 1.2881\ \rho_{old}$ (the total amount is conserved);
3) Graphite density used: 0.0708873 a/cm b (adjusted).

The following table presents the results for the whole reactor.

Model Config.	DIF3D (diffusion) hexagonal Model 1	DIF3D (transport) hexagonal Model 1	MCNP hexagonal Model 2	MCNP (mixed, real reflector) Model 3	Error Model 1 (diffusion) vs. Model 3	Error Model 1 (transport) vs. Model 3	Error Model 2 vs. Model 3
UPP	1.06012	1.06810	$1.05922 \pm 0.14\%$	$1.05571 \pm 0.10\%$	Δk=0.441%; Δρ=394 pcm	Δk=1.239%; Δρ=1098 pcm	Δk=0.351%; Δρ=314 pcm
NOM	1.01872	1.02601	$1.02264 \pm 0.13\%$	$1.01389 \pm 0.10\%$	Δk=0.483%; Δρ=468 pcm	Δk=0.375%; Δρ=360 pcm	Δk=0.875%; Δρ=844 pcm

Table 3 Results for the whole core after the appropriate adjustments of the reflector's materials

Finally we note that we also used the code DRAGON to compare the cross sections obtained with WIMS. The cross sections from both codes give similar results when used in DIF3D.

The proposed above adjustment does not constitute the final and unique value of the graphite density. It is clear that such an adjustment should be made taking into consideration the analysis for as many as possible critical configurations. We reserve the possibility to improve this value, as new information about this specific TRIGA's geometry/composition becomes available.

III.3.3 Reaction rates and power density distributions distribution

We used DIF3D code (transport, VARIANT option) and resulted NHFLUX file to reconstruct the reaction rates at several locations in the core in the UPP configuration. In Figure 12 we schematically show the radial location of the detectors. In radial direction the detectors are located at the following distances from the core center X = 3.465, 7.830, 12.195, 16.560, 20.925 cm. In axial direction (MCNP geometry) the detectors are located in the fuel zone of assemblies at Z = 19.42, 27.04, 34.66, 42.28 cm. The fuel section of the TRIGA pin runs from 11.8 to 49.91 cm in axial direction. In the reference where the bottom of the pin fuel zone is taken for zero the axial partition is Z = 7.62, 15.24, 22.86, 30.48. In radial directions the detectors are named d1 through d5. We simulated the ^{235}U fission chambers with detectors' cross sections taken from the ISOTXS file (^{235}U in the fuel cross sections in 9 groups). All the detectors are located in the fuel zone except for the detectors in the '5 series' (first index is 5). These are located in the TRIGA regulation rod. In the UPP configuration the regulation rod is 50% inserted in the core. The results of our calculations are shown in the Figure 14. The reaction rates are normalized to unity (divided by the sum of reaction rates at different positions). We note the drop in the fission rate values in detectors d4 and d5 at higher Z positions. This is related to the proximity of the regulation rod.

We also reconstructed the axial and radial power density distribution as calculated by the DIF3D code. The assemblies chosen to establish radial distributions are the same as for the reaction rates. We divided the fuel section of each assembly in five regions 7.622 cm high. The lower fuel region point is 21.8 cm, the highest is 59.91 cm. The

Figure 15 and Figure 16 illustrate our results. The points in the Figure 16 indicate the lowest boundary of the axial cut regions.

III.3.4 Analysis of the recent critical configurations (Fall 2002)

A number of critical configurations of the TRIGA reactor were recently realized (see chapter IV). These critical configurations served to choose the appropriate reference for the reactivity measurements detectors types, and to estimate the worth of control rods and central elements of the core. The following table describes the 4 critical configurations.

	CONTROL RODS POSITIONS			
	SH1 (C10)	SH2 (C7)	SEC (C4)	REG
CRITICAL 1	UP	UP	UP	751/800
Critical 1 notes	1) 2 assemblies (positions B1 and B5) are voided starting at the lower graphite section of a fuel pin up to 40 cm above the core with void diameter of 2.54 cm 2) 2 assemblies (positions B2 and B4) are filled with water			
CRITICAL 2	UP	DOWN	UP	402/800
Critical 2 notes	1 assembly (position B5) is voided up to 40 cm above the core			
CRITICAL 3	481/800	DOWN	UP	UP
Critical 3 notes	Core restored to normal			
CRITICAL 4	665/800	DOWN	UP	DOWN
Critical 4 notes	A graphite element (G19) is removed and the position is filled with water			

Table 4 Description of the recent critical configurations of the TRIGA reactor.

We used three different codes to assess the k_{eff} of these configurations: to the previously used MCNP and DIF3D, the code ERANOS was added. This is done for the future calculations of MSM factors for which the ERANOS has an established procedure. We remind that in DIF3D and ERANOS the density of material in the reflector was adjusted as described in the previous section. To take into account the voided elements we decreased the water density in the corresponding assemblies. In the critical configuration 1 the void was 'distributed' between assemblies B1, B2, B4 and B5, resulting in the following adjustment of the water density $\rho_{new} = 0.8553\ \rho_{old}$. In the critical configuration 2, the void was 'distributed' in the B5 assembly only resulting in the following adjustment of the water density $\rho_{new} = 0.7107\ \rho_{old}$.

The following table presents the k_{eff} for described above configurations.

	MCNP (mixed, real reflector) Model 3	MCNP (all real geometry model 4) ANL compositions from Ref. 5	DIF3D (diffusion)	ERANOS (diffusion)
CRITICAL 1	$1.02973 \pm 0.15\%$	$1.03206 \pm 0.10\%$	1.03117	1.03188
CRITICAL 2	$1.02441 \pm 0.14\%$	$1.02435 \pm 0.11\%$	1.02744	1.02972
CRITICAL 3	$1.02330 \pm 0.15\%$	$1.02371 \pm 0.11\%$	1.02665	1.02749
CRITICAL 4	$1.02776 \pm 0.13\%$	$1.02521 \pm 0.10\%$	1.02839	1.02744

Table 5 Results of the analysis of the four TRIGA critical configurations with MCNP, DIF3D and ERANOS codes.

It is seen that the results for all codes used are consistent. Nevertheless, they exceed predicted experimental values of k_{eff}=1 by 2.3-3%. This might signify that the information available at the moment for TRIGA reactor's composition/geometry is not adequate.

To find the origin of the high k_{eff} values, we used the detailed fuel composition (available at ANL, Ref. 5) for the critical configuration 1in the MCNP with all real geometry. The resulting k_{eff}=$1.02235 \pm 0.11\%$. This is in very good agreement with the CEA results obtained for this configuration with the Monte-Carlo code TRIPOLI (Ref. 7).

Moreover, the detailed examination of the previous work (Ref. 5) and communication with the ENEA (Ref. 6) showed that the detailed compositions for the fuel pins and absorbers in TRIGA used at ANL (Ref. 5) and ENEA (Ref. 6) are slightly different. This is due to the rounding of the numbers. Also, the absorber weight fractions are different in both cases:

ANL (conform to the Excel file distributed to the TRADE participants, Ref. 5):
B10 0.079
B11 0.351
C 0.57.

ENEA (Ref. 6):
B10 0.0989
B11 0.4011
C 0.5.

The geometry model of the TRIGA reactor is also different, in particular on the following potentially important points:

1. The absence of the modeling of the upper (above the core) control rods by ENEA when the rods are partially withdrawn.
2. Presence of the two voided vertical channels above the graphite reflector.

We used our all real geometry MCNP model with the ENEA detailed compositions (fuel and absorbers) to analyze the critical configuration 1. The resulting $k_{eff}=1.02021 \pm 0.09\%$. The value reported by the ENEA is $1.01887 \pm 0.02\%$. The agreement between these two calculations is fairly good. We mention that ENEA description of the experiment is probably more detailed than reported in the present work (the detectors and the aluminum tubes were modeled in detail in voided assemblies, Ref. 6). Nevertheless, there still exist doubts about the fuel compositions. The origin of the mentioned above informational discrepancies is being investigated.

III.3.5 The calculation of the MSM factors

Here a brief description of MSA (méthode de source approchée, approximated source method) and its corrector MSM (méthode de source modifiée, modified source method) to experimentally determine the reactivity is given.

From the point kinetics equations the relation between the reactivity ρ, neutron population N, prompt neutron life-time Λ and the external neutron source Q is:

$$\rho = -\Lambda Q / N . \qquad (1)$$

The neutron population and prompt neutron life-time can be expressed in terms of ϕ_0^* (adjoint flux in corresponding critical system) and Ψ (form-factor of flux in subcritical system) by:

$$N = \left\langle \phi_0^*, \frac{1}{\upsilon}\Psi \right\rangle \text{ and } \Lambda = \frac{\left\langle \phi_0^*, \frac{1}{\upsilon}\Psi \right\rangle}{\left\langle \phi_0^*, F\Psi \right\rangle},$$

where F is fission operator. With these expressions the reactivity is determined as follows:

$$\rho = -\frac{Q}{T_d}\frac{\left\langle \Sigma_d, \phi_s \right\rangle}{\left\langle \phi_0^*, F\phi_s \right\rangle}. \tag{2}$$

In the last formula we introduced the reaction rate in the detector as: $T_d = \left\langle \Sigma_d, \phi_s \right\rangle$.

Therefore, the MSA reactivity can be expressed as:

$$\rho = -\frac{\varepsilon Q}{T_d} \text{ with } \varepsilon = \frac{\left\langle \Sigma_d, \phi_s \right\rangle}{\left\langle \phi_0^*, F\phi_s \right\rangle}. \tag{3}$$

In other words, if Q and ε are constant, the reactivity in a subcritical system is inversely proportional to the reaction rates in the detector. Obviously, the values of Q and ε cannot be detected experimentally. Thus, to measure the reactivity by MSA method one must gauge it with the known reactivity of a known configuration. Suppose that we know the reactivity ρ_1 corresponding to the detector rate T_{d1}, therefore by calibration the desired reactivity can be expressed as:

$$\rho = \frac{T_{d1}}{T_d}\rho_1, \tag{4}$$

where the gauge coefficient is the ratio of detector rates in two configurations.

It is clear that the last expression (MSA expression for the reactivity) is directly applicable to the measurement of the reactivity. However, it was obtained in the framework of point kinetics. It is possible to correct the obtained above results by taking into account spatial effects.

Consider the inhomogeneous transport equation for a system with an external source:

$$(F - A)\phi_s + Q = 0, \tag{5}$$

where A is the destruction operator and ϕ_s is the flux in the system. The corresponding critical real and adjoint equations are:

$$\begin{aligned} (F/k_{eff} - A)\phi_0 &= 0, \\ (F^*/k_{eff} - A^*)\phi_0^* &= 0, \end{aligned} \tag{6}$$

where k_{eff} is the multiplication factor in a critical system. If we multiply the equation (5) by ϕ_0^* and integrate over energy and space, we obtain:

$$\rho = -\frac{\left\langle \phi_0^*, Q \right\rangle}{\left\langle \phi_0^*, F\phi_s \right\rangle}.$$

Now we introduce the detector reaction rate in the last expression $T_d = \left\langle \Sigma_d, \phi_s \right\rangle$ and directly obtain:

$$\rho = -\frac{\varepsilon S}{T_d}, \tag{7}$$

with ε once again expressed as $\varepsilon = \frac{\left\langle \Sigma_d, \phi_s \right\rangle}{\left\langle \phi_0^*, F\phi_s \right\rangle}$ and $S = \left\langle \phi_0^*, Q \right\rangle$. In the MSM expression for the reactivity (7), the detector efficiency ε depends on the detector's nature and its position.

As compared to the MSA method, the expression (7) takes into account special effects. In the same fashion as in the case of MSA method, one obtains a gauge expression for the reactivity ρ in terms of known parameters ρ_1, T_{d1}, ε_1 and S_1 of a know (reference) configuration:

$$\rho = \rho_1 \frac{T_{d1}}{T_d} \frac{\varepsilon}{\varepsilon_1} \frac{S}{S_1}. \tag{8}$$

The ration $\xi = \frac{\varepsilon}{\varepsilon_1} \frac{S}{S_1}$ is the MSM efficiency correction factor that takes into account the variation of the source and the differences in neutron flux distributions between the reference and desired configurations.

Now, we will apply these expressions to calculate the MSM factor for the TRIGA critical configurations described in the previous chapter. Despite the high values of the multiplication factors calculated in the previous chapter as compared to the experiment, one can estimate the MSM factors since they depend on the ratios of weighted reaction rates. Therefore, unless the local flux shape at detectors positions in the reactor changes significantly, the higher than experimental values of k_{eff} will not affect the MSM factors.

We used the code ERANOS to calculate the MSM factors. The critical configuration 4 was used as a reference as the experimentalists requested it. The external neutron source is the Am-Be source in the position F24. The source is a hexagon prism (standard TRIGA hexagon with the height of 5.5 cm) situated at the center of the source assembly. The intensity of the source is 1.4E7 n/s, which results in the total neutron flux for the chosen source volume of ~1.5426E5 n/s cm^3. The energy spectrum was taken from Ref. 8 and adapted to the 9-group structure described previously. In fact there are only two high-energy components relative to our group structure: 0 to 5E5 eV with a yield of 0.066, and 5E5 to 1E7 eV with a yield of 0.934.

In order to make the system subcritical in all four configurations, we adjust the fission spectrum by the highest k_{eff} value as given by a transport calculation. This highest k_{eff}=1.03188 is the value for the configuration 1 in diffusion approximation. The corresponding transport calculation for this configuration gives k_{eff}=1.0359459. Therefore,

we adjust the fission spectrum in all configurations by the factor 0.96. This results in the following multiplication factors (subcritical) as calculated with transport option of ERANOS.

	CRITICAL 1	CRITICAL 2	CRITICAL 3	CRITICAL 4
ERANOS transport k_{eff}	0.994508	0.989553	0.988805	0.989927
ERANOS subcriticality	-552 pcm	-1056 pcm	-1132 pcm	-1018 pcm

Table 6 Subcriticality level in 4 TRIGA critical configurations after the fission spectrum adjustments as calculated with the VARIANT (transport) option of the ERANOS code.

As mentioned above the critical configuration 4 was taken as a reference for the MSM factors calculation. The MSM factors were calculated at centers of the lattice's hexagons (pitch 4.365 cm) at the axial point z=30 cm (8.2 cm above the start point of the TRIGA's fuel, which runs from 21.8 to 59.91 cm). The diagrams in Figure 17, Figure 18, and Figure 19 schematically show the TRIGA's core with radial MSM traverses.

III.3.6 The calculation of the MSM factors with all control rods inserted.

The experimental team at ENEA, Italy also requested a set MSM factors calculations for the recent critical configurations *with all control rods inserted into the core*. The same configurations/codes/geometries/composition are used in this chapter for the four critical configurations with the only exception that all control rods were completely inserted into the core as requested by the experimentalists. All the calculations were performed in a way consistent with the description given in the previous chaptwer. The corresponding multiplication factors for the four critical configurations with all control rods inserted are given in the following table:

	CRITICAL 1	CRITICAL 2	CRITICAL 3	CRITICAL 4
ERANOS transport k_{eff}	0.915277	0.930790	0.934357	0.934028
ERANOS subcriticality	-9257 pcm	-7436 pcm	-7025 pcm	-7063 pcm

Table 7 Subcriticality level in 4 TRIGA critical configurations with all control rods inserted as calculated with the VARIANT (transport) option of the ERANOS code.

The MSM factor for the detectors positions is the following.

CRITICAL 1:

Detector in B1 MSM(B1)=1.8819
Detector in B5 MSM(B5)=1.9795

CRITICAL 2

Detector in B5 MSM(B5)=1.6338

III.4 Conclusion

In this section we presented the deterministic analysis of the TRIGA reactor with the DIF3D code. We showed that the straightforward transformation of the TRIGA's geometry into hexagonal model yields large discrepancies between Monte Carlo calculations and DIF3D diffusion and transport calculations. In order to remedy this disagreement it was shown that an adjustment of the graphite reflector density is the best option. Using this adjustment, one obtains good agreement with the Monte Carlo calculations.

Further, using MCNP code we analyzed the series of recent experiments performed in TRIGA in fall 2002. The calculated multiplication factors do not agree with experiment and differ from it by 2000-3000 pcm. These results are consistent with the partial analysis performed by ENEA and CEA (Ref. 6 and 7). We deduce that there exists a bias as to the exact fuel/absorber compositions reported by the ENEA for TRIGA. A proper burnup calculation might be in order to address this issue. The creation of the hexagonal model allows for easy calculation of the MSM factors with the ERANOS code. We calculated the MSM factors for the three recent critical configurations of the TRIGA reactor.

IV. First Results from Phase IA Experiments in Fall, 2002

IV.1 Introduction

The Phase IA (initial) experiments began on 18 November, 2002 at the TRIGA reactor at the Casaccia Center near Rome. A CEA/ANL team of three persons came from the Cadarache Centre in France, bringing assorted electronic equipment in a van (computer data acquistion, pre-amps and amplifiers, power supplies, etc.). This early part of the phase IA experiments had the following broad objectives:

- Chamber checkout
- Reactivity worth of fuel elements and graphite elements
- Flux estimation
- Control rod calibrations
- Temperature feedback of reactivity

The CEA/ANL group stayed a week, and assisted in the completion of the first three items above. The ENEA staff then completed the other tasks in the following two weeks. The purpose of this report is to document the information obtained during the period of experiments.

IV.2 Chamber Checkout

There are over 30 BF_3 proportional counters at the TRIGA facility in Casaccia, which had been obtained from a shutdown reactor in Bologna. The chambers are old (more than 20 years), but it was believed that most of them would be operational. The sensitivities range from 0.065 cps/nv to over 20 cps/nv. The purpose of this testing was to see if any of these chambers could be used in lieu of new fission chambers for the MSA measures.

To begin the measurements, four fuel elements from the B-ring were removed, specifically B-1, B-2, B-4, and B-5 This configuration is shown in Figure 20. Note that the numbering system starts with B-1 being in the same azimuthal position as the regulating (REG) rod in the F-ring, and the numbering order in each ring is clockwise. We began the measurements with the chamber 5B40/13, a chamber with a nominal active length of 5cm and an outside diameter of 1.3cm. Its sensitivity is about 0.065 cps/nv.

The CEA electronic chain was used, which includes a PC based PHA which allows easy discrimination of background counts due to gammas (and alphas in the case of fission chambers). The first configuration tested was with all control rods down, and chambers were placed in B-1, B-4, and B-5. All three of these chambers produced 80% dead time, with count rates on the order of 180,000 cps. A test was then performed by raising the safety rod, which would add over \$2.00 (1500 pcm[1]) reactivity to the sub-critical core. Essentially we did not see any increase in the counts from any of the three chambers, which indicates that they were well saturated in these positions in the core.

We then performed a number of tests over the period of two days. We removed the source, we moved the detectors close to the source, we tried covering the detector with cadmium to desensitize it, etc. In spite of these attempts, we basically concluded that the BF_3 detectors are much too sensitive for use in MSA (a technique for estimating subcritical reactivity by source multiplication). This is not entirely unexpected as they are operated as proportional counters, which increases their sensitivity to gammas. At any rate, these chambers could be used for monitoring outside the core (and fixed reflector), but they are not suitable for the in-core monitors planned for MSA in TRADE.

We then tested the miniature (1.5ϕ mm) fission chambers that were also at the TRIGA facility. These chambers are of CEA origin, and are roughly 20 years old. According to the records, there were supposed to be two U-235 chambers, one U-238 chamber, one Pu-239 chamber, and one Np-237 chamber. Since the preferred isotope for a monitoring fission chamber in TRADE is U-235, we began by testing one of the U-235 chambers. Unfortunately, this chamber did not respond at all, so the other supposed U-235 chamber was tested. For this chamber, a good fission fragment pulse shape was observed, but at a much reduced count rate (in fact, a count rate more typical of a U-238 chamber in a water reactor). It was later discovered that the chamber was indeed mismarked, and is in fact a U-238 chamber. We then tested the other U-238 chamber, and found that it worked as well. Finally, we tested the Pu-239 chamber, and found that it performs very well, so we used that chamber for some other flux measures. Due to lack of time, we did not test the Np-237 chamber.

Thus, the final inventory of chambers tested is:

- BF_3 chambers work, but too sensitive
- No working U-235 chamber
- Two working U-238 chambers
- One working Pu-239 chamber
- Np-237 chamber is un-tested

[1]Throughout this report, β is taken to be 0.0075, or 750 pcm

IV.3 Reactivity Estimates

The next series of experiments dealt with obtaining estimates of reactivity worths of fuel elements. This information will help in the decision regarding the immediate purchase of fresh fuel for the reactor.

We began with the configuration that existed after the chamber testing experiments. That is, the same four B-ring elements removed, the Pu-239 chamber in position B-5, and a BF_3 chamber in position B-1. Positions B-5 and B-1 could be considered as voided with a diameter of 1 inch, while positions B-2 and B-4 were completely water filled (Figure 20).

The two shim rods (SH1 and SH2), and the security rod (SEC) were removed; and the regulating rod (REG) was removed until the reactor achieved criticality. Criticality was obtained at a REG rod position of 751/800, i.e., nearly fully withdrawn. A doubling time measurement was made by completely withdrawing the REG rod, and it was found that the reactor had only 3.8¢ of excess reactivity[2] .

The excess reactivity of 3.8¢ (29 pcm) in this configuration can be accepted with a high degree of confidence: there are no control rod interaction effects (all rods are out), and the reactor has so little excess that the doubling time is very long. We then made an estimate of the shutdown reactivity (all rods inserted) by performing rod-drops of each control rod. The control rod worth from the rod drop was estimated in two ways: 1) by examining the ratio of $n(t)/n(0)$ at times of 5, 10, and 15 seconds and using the data from GA (Figure 21) to estimate the reactivity, and 2) by examining the prompt drop as follows.

Point kinetics predicts that there will be a prompt drop in the neutron population following a rapid insertion of negative reactivity. The drop is given by

$$\Delta = \frac{n}{n_0} = \frac{\beta}{\beta - \rho}.$$

Because the reactivity in dollars is given by ρ/β, we can write that the reactivity in dollars after a prompt drop is given by

$$\$ = 1 - \frac{1}{\Delta}$$

The reactor strip chart recorder was set to high speed (1 division equals 1 second) just before the drop. Copies of the charts are shown in Figure 22, Figure 23, Figure 24, and Figure 25. In addition the chart from dropping all four rods at once is shown in Figure 26. Both the ratio at 5 seconds and the prompt drop were examined using the data on these charts, and the results are summarized in Table 1.

[2]Note that SEC, SH1, and SH2 are fuel followed control rods. With them fully withdrawn, the core is relatively clean from an axial perspective, i.e., there is no partially inserted high worth control rod. Thus, this configuration very near critical could be used as a benchmark.

	Prompt Drop	5 sec Inverse Kinetics	Past (full core)
SH1	2.10	1.80	2.98
SH2	1.97	1.73	3.06
SEC	2.27	2.10	3.78
REG	0.63	0.53	0.76
SUM	6.97	6.16	10.58
4 rods	5.53	NA	NA

Table 8 Estimates of control rod worths—values in $

We noticed several items as we examined the chart recorder data. First, when estimating reactivities we noticed that the predictions of the amount of reactivity decreases with time after the drop. That is, the prediction using the ratio at 10 seconds is always less than the prediction at 5 seconds, and the same for 15 seconds versus 10 seconds. This indicates that the neutron population is not decreasing at a rate predicted by point kinetics, and in fact is decreasing at a lesser rate. This is consistent with the effect of a background source, but we must perform more measurements to determine if the background source is indeed non-negligable.

The second point is seen directly from Table 8 - that is, the reactivity predictions using the 5 second inverse kinetics values are always lower in magnitude than those predictions using the prompt drop method. Normally, we would expect the 5 second method to be more reliable because it is based on 6 delayed groups of neutrons, and the stable period is achieved after a few seconds. For the prompt drop, we must remember that the control rod takes a finite time to fall completely (less than 0.5 seconds), so the prompt drop will be somewhat contaminated by this effect. In any case, the differences between the two methods are on the order of 10-15%, which allows us to attach a very crude estimate of uncertainty to these measures.

For the third point, shown dramatically and consistently by all methods, we can see from Table 8 that there has been a loss of control rod worth of the order of four dollars in this configuration. This is consistent, because the control rods are in the C-ring, and surely will lose worth with the removal of B-ring fuel elements.

For the moment, lacking better experiments, we are assuming that the estimated control rod worth is the average of the prompt drop and 5 second inverse kinetics. Thus, in Table 9 we show the current best estimate of rod worth, the past (1998) value, the percentage difference between the values obtained via prompt drop versus the 5 second inverse kinetics (deviation), and the loss in rod worth caused by the removal of the four B-ring elements.

	Best Estimate	Past (full core)	Loss	Deviation
SH1	1.95	2.98	1.03	14%
SH2	1.85	3.06	1.21	12%
SEC	2.19	3.78	1.59	7.5%
REG	0.58	0.76	0.18	16%
SUM	6.57	10.58	4.01	12%

Table 9 Best estimates of control rod worths—values in $

We can now summarize the first configuration of 4 B-ring elements removed with two positions taken by detector housing tubes and two water filled. For control rod worth, we are

ignoring rod interaction effects. This is adequate for these very preliminary measures. More precise determinations of reactivity will have to wait for the delivery of the fission chambers for MSA.

- core excess $0.04 (29 pcm)
- control rod worth $6.57 (4928 pcm)
- core subcriticality $6.53 (4899)

We are thus estimating that the core sub-criticality with 4 B-ring elements removed and all control rods inserted is about 4900 pcm, or k~0.95. This was extremely fortuitous since this is within the planned operation range of the TRADE experiments.

For the second configuration, three of the B-ring elements were replaced, leaving the Pu-239 chamber and its housing in location B-5 (we used this chamber to test MSA/MSM techniques knowing full well that it will be a challenge to obtain the correction factors in such a configuration). Now, with most of the core restored to normal, we used the control rod calibrations of the full core to make estimates of reactivity. We would obtain the reactivity worths using at least two different rod patterns to establish consistency. The rod positions for criticality in configuration 2 are shown in Table 10.

SH1	SH2	SEC	REG	Excess ($)
Up	Down	Up	402 (late afternoon)	3.60
Up	Down	Up	407 (next morning)	3.59
Up	226	Up	Down	3.55

Table 10 Critical rod positions for configuration 2

From Table 10 we see a very good repeatability in estimated excess from one day to the next (within 1 cent, or 7 pcm), and good consistency with two different critical configurations (4 cents, or about 29 pcm).

We now compare our estimated excess of $3.58 (average of the three separate estimates) to that with four B-ring elements removed ($0.04). We can thus estimate that the worth of three fuel elements versus two void locations and one water filled location is $3.54 (2655 pcm).

The third configuration was a return to the full core—that is, the detector and housing were removed from B-5 and the fuel element restored to its normal position. The rod positions for criticality are given in Table 12.

SH1	SH2	SEC	REG	Excess ($)
481	Down	Up	Up	4.36
Down	472	Up	Up	4.42
Down	583	Up	Down	4.48

Table 11 Critical rod positions for configuration 3—normal core

The average excess given in Table 11 is $4.42, and comparison to the excess of $3.58 in configuration 2 implies a B-ring fuel element worth of $0.84 compared to void/detector.
A G-ring fuel element was then removed to yield the fourth configuration. The rod positions for criticality are given in Table 12.

SH1	SH2	SEC	REG	Excess ($)
665	Down	Up	Down	4.15
Down	625	Up	Down	4.20
Down	508	Up	Up	4.12

Table 12 Critical rod positions for configuration 4

The average excess implied by Table 12 is $4.16, and thus the worth of the G-ring element versus water is $0.26. A subsequent experiment demonstrated that the worth of a G-ring graphite element versus water is about $0.08.
We summarize the measurements in Table 13.

Config	Excess ($)	S.D. ($)	S.D. (pcm)
4 B-ring	0.04	6.53	4900
1 B-ring	3.58	7.00	5250
Full core	4.42	6.16	4620
G-ring	4.16	6.42	4815

Table 13 Summary of reactivity estimates

It is interesting to note from Table 13 that the shutdown reactivities (level of subcriticality) always range from 4500-5000 (a multiplication factor around 0.95). It is the excess reactivity that changes the most from configuration to configuration, and not the level of subcriticality with all rods inserted.

IV.4 MSA

It is not feasible to use the count rates directly from the detector in position B-5 for estimation of sub-criticality by MSA methods. The perturbation from the removed adjacent fuel and nearby control rods is too great. However, data were accumulated, and we hope to be able to make better estimates when the MSM factors are calculated.

Nevertheless, we show the data recorded by the Pu-239 chamber during the rod drops in the first configuration (for four B-rings removed) in Figure 27-Figure 30. We attempted to use this data to estimate the 5, 10 and 15 data for the use in Figure 21, and also to estimate the prompt drop. It is clear that the drop of SH1 creates a great perturbation in neutron population as seen by the detector in position B-5 (note that the detector and SH1 are very close). This is seen dramatically in Figure 28, the drop of SH1 alone, but also in Figure 31, which is the drop of all four rods.

IV.5 Flux Estimates

The Pu-239 chamber that we used had been calibrated in MOL in 1984 and again in 1986 to obtain an effective fissionable mass. For the Pu chamber, the effective mass is given as 23.6 μg of Pu-239. Other impurities can be ignored because of the dominance of the fissile isotope. Although this effective mass was determined in a fission spectrum, studies of effective masses obtained in a fast spectrum and used in a thermal spectrum have shown that the results are spectral independent (Ref. 9). We are using these data to estimate the efficiency of the fission chambers that will be used for future MSA/MSM measures of reactivity.

We made a measure of the flux at the edge of the core in the fourth configuration (B-ring filled with fuel, one G-ring element removed and the detector in that position). As shown in Table 13 , the shutdown reactivity is about 4700 pcm, so we are near k=0.95. To first order, one can assume that all fissions occuring in the lightly loaded chamber result in one count. In the fourth configuration, with all four control rods down, we measured 1.7 cps in the Pu-239 chamber. This implies approximately 7.2×10^4 fissions/second/gram. Now, the reaction rate in normalized fissions/second/gram can be written as:

$$R_M = \frac{0.6023\sigma\phi}{239}.$$

Thus, for Pu-239, $R_M = 1.9\phi$, and 1.7 cps implies a flux of about 4×10^4 n/cm^2/sec.
To estimate the sensitivity of the detector desired, assume that the peak count rate wanted near critical (100 pcm) is 20,000 cps. This will imply a count rate of around 400 cps at k=0.95 assuming there are not gross changes to the core geometry between those two states. At k=0.95, we measured a flux of around 4×10^4. Thus, a detector of efficiency around 0.01 cps/nv will yield the target count rates in the range between 100 to 5000 pcm of reactivity[3] .

IV.6 Control Rods Calibration

The TRADE experiment represents a fairly major perturbation to the TRIGA core, and it is possible that there will be perturbations to the kinetics constants. It is certain that the control rod worths will change. Because of this, it was desirable to re-calibrate the control rods in the normal state of the core before the transition to the TRADE reference core is made. At the same time, an automated procedure, derived from the practice currently used in the periodic control rod calibrations, was assessed. It is based on a PC integrated with the old (standard) reactor instrumentation.

For this purpose, the signal derived from one of the two compensated ion chambers (located outside the reflector) and exiting a linear electrometric amplifier (already used for the paper chart recorder) was connected to an A/D card in the PC.

A LabView© program was designed for the acquisition of the signal related to the neutron flux during the divergences. At the end of the acquisition, the program performs the evaluation of period τ and reactivity ρ using the inhour equation:

$$\frac{\Delta\rho}{\beta_{eff}} \approx \frac{\ell}{\beta_{eff}\tau} + \sum_{i=1}^{6} \frac{f_i}{1+\lambda_i\tau}$$

This relationship can be applied with $k \approx 1$. τ is the stable period of the reactor (Ref. 10).
We assume the thermal neutron average lifetime ℓ is 80 μs, β_{eff} is 0.0075, and the values reported in Table 14 for the six delayed neutron groups.

[3]It should be noted that this efficiency is only estimated with MSA in mind. Planned noise techniques will require chambers with much greater sensitivities.

Group	f_i	λ_i
1	0.033	0.0124
2	0.219	0.0305
3	0.196	0.1115
4	0.395	0.301
5	0.115	1.138
6	0.042	3.01
Σ	1.000	

Table 14 Delayed neutron groups

The results of the control rod calibrations (Figure 32-Figure 35) demonstrate the classical S-shape of the reactivity curves and in fact the shapes and the measured total reactivities are in good agreement with the measurements performed three years ago[4] . The system described will be useful when new sets of β and λ values are assessed after the kinetics measurements in the future configurations.

IV.7 Reactivity Coefficient

The main TRIGA attribute, the prompt negative reactivity coefficient, is related to the design of the fuel element (Ref. 11). Special experimental setups were arranged by General Atomic during the design activities of the TRIGA in order to assess the prompt temperature coefficient.

The delayed temperature coefficients, which arise mainly from the heating of the water as it is circulating between fuel elements that are experiencing a temperature surge, are negligible compared to the prompt coefficient. The total temperature coefficient, the *bath coefficient*, is a combination of the two types of coefficients but is dominated by the prompt part coming directly from fuel heating.

The configuration of ENEA's TRIGA RC-1 and the availability of only a single instrumented fuel element, combined with the licensing constraints that do not permit the handling of the instrumented fuel during reactor operation, allow only an estimation of the bath coefficient. With the above considerations, we can assume that it is ascribed to the prompt temperature coefficient.

The procedure for estimating this coefficient, regularly used by the reactor staff for periodical checks, is based on the insertion of a known positive reactivity (10-15¢). Normally, the staff starts from a steady state power of 10 W. Fuel temperature and power are recorded during the transient with the system described in section IV.6. A new steady state is reached, the level of which directly depends on the temperature coefficient effect. The power evolution after such a reactivity insertion is shown in Figure 36.

The energy inside the total number of fuel elements is evaluated by integrating the power with respect to time, from the beginning of the step to the final steady power limited by the temperature coefficient. This is shown in Figure 37.

[4]For example, see Table 9. This shows a loss of 2¢ for SH1 and SH2, a loss of 1¢ for SEC, but a gain of 5¢ for REG. Thus, the net change is zero.

Assuming that fuel prompt coefficient dominates, and with the knowledge of the fuel heat capacity, the related temperature increase is evaluated. The ratio between the reactivity step and the temperature increase value gives the prompt temperature coefficient.
The fuel specific heat capacity is evaluated as:

$$C(T) = 2.57 \times 10^6 + 2940 \times T$$

Note that the total heat capacity includes the Zr rod inside the fuel element (Ref. 12). The core volume consists of the loaded fuel elements plus the fuel part of the control rod inserted in the core.
The core mean temperature is calculated as

$$\overline{T} = \frac{T_{mean}(1MW)}{T_{B6}(1MW)} T_{B6},$$

$T_{mean}(1MW)$ is the mean temperature of the entire core elements at 1 MW, $T_{B6}(1MW)$ is the fuel temperature (at 1 MW) in B6 position, and T_{B6} is the mean value of the temperature measured during the power transient.
The temperature increment is:

$$\Delta T = \frac{E}{C(T)}$$

The reactivity coefficient is calculated as:

$$|\alpha| = \frac{\Delta k}{\Delta T} \beta \times 10^5$$

where Δk is in pcm. The sequence "power step-new steady state" was repeated at different powers ranging from 20 W to 900 kW. The plot of the prompt reactivity coefficient and temperature of fuel and water versus the reactor power is shown in Figure 38. A second order polynomial fit for the reactivity coefficient is also given with the following parameters:

A	-3,9
B1	-0,08
B2	3,081E-5

IV.8 Conclusion

The broad objectives of the early Phase IA experiments were met. Some of the items important for characterization of the TRADE reference configuration (such as control rod worths and reactivity temperature coefficients) were obtained with satisfactory precision. Other parameters such as reactivity worths in severely perturbed conditions (e.g., four B-ring elements removed) were obtained with less precision. Improvements in measurements of these parameters depend on two items being completed:

- delivery of fission chambers to Casaccia
- calculation of MSM factors for the TRIGA

These are required prior to commencing the next segment of Phase IA.

IV.9 Acknowledgements

We are indebted to the TRIGA operations staff at Casaccia Centre for their cooperation and interest during the conduct of this work. These experiments could not have been performed on schedule without their hard work and competence in reactor operations.

V. Conclusions

Several conclusions can be drawn from the study presented in this report.

The TRADE experiment represents a necessary step in the process of validation of the ADS concept, the next step being the demonstration of the waste transmutation in a prototypical ADS. The representativity of the experiment has been discussed. The fact of having a thermal neutron spectrum and an external source due to relatively low energy E_p=100 MeV protons is not significant in terms of the overall validation of the dynamic behaviour of an ADS in different regimes ("source" – dominated, "core feedback" – dominated), of the start-up and shut-down procedures, of the monitoring of reactivity variation during irradiation etc. Moreover, the "full scale" demonstration of the coupling of the real components (accelerator, target, subcritical core) will bring invaluable elements to future ADS engineering designs. The TRADE experiment should then provide already by end of 2006 and beginning of 2007, first relevant elements of demonstration of the ADS concept. The successive campaign of experiment should consolidate and enlarge the experimental validation data base.

The deterministic analysis of the TRIGA reactor with different codes was also presented. We showed that the straightforward transformation of the TRIGA's geometry into hexagonal model yields large discrepancies between Monte Carlo calculations and DIF3D diffusion and transport calculations. In order to remedy this disagreement it was shown that the adjustment of the graphite reflector density is the best option. Using this adjustment one obtain a good agreement with the Monte Carlo calculations. Moreover, using the MCNP code we analyzed the series of recent experiments performed in TRIGA in fall 2002. The calculated multiplication factors do not agree with experiment and differ from it by 2000-3000 pcm. These results are consistent with the partial analysis performed by ENEA and CEA (Ref. 6 and 7). We deduce that there exists a bias as to the exact fuel/absorber compositions reported by the ENEA for TRIGA. A proper burnup calculation might be in order to address this issue. The creation of the hexagonal model allows for easy calculations of the MSM factors with the ERANOS code. We calculated the MSM factors for the three recent critical configurations of the TRIGA reactor.

The broad objectives of the initial phase experiments were met. Some of the items important for characterization of the TRADE reference configuration (such as control rod worths and reactivity temperature coefficients) were obtained with satisfactory precision. Other parameters such as reactivity worths in severely perturbed conditions (e.g., four B-ring elements removed) were obtained with less precision. Improvements in measurements of these parameters depend on two items being completed:

- delivery of fission chambers to Casaccia
- calculation of MSM factors for the TRIGA

These are required prior to commencing the next segment of the initial phase.

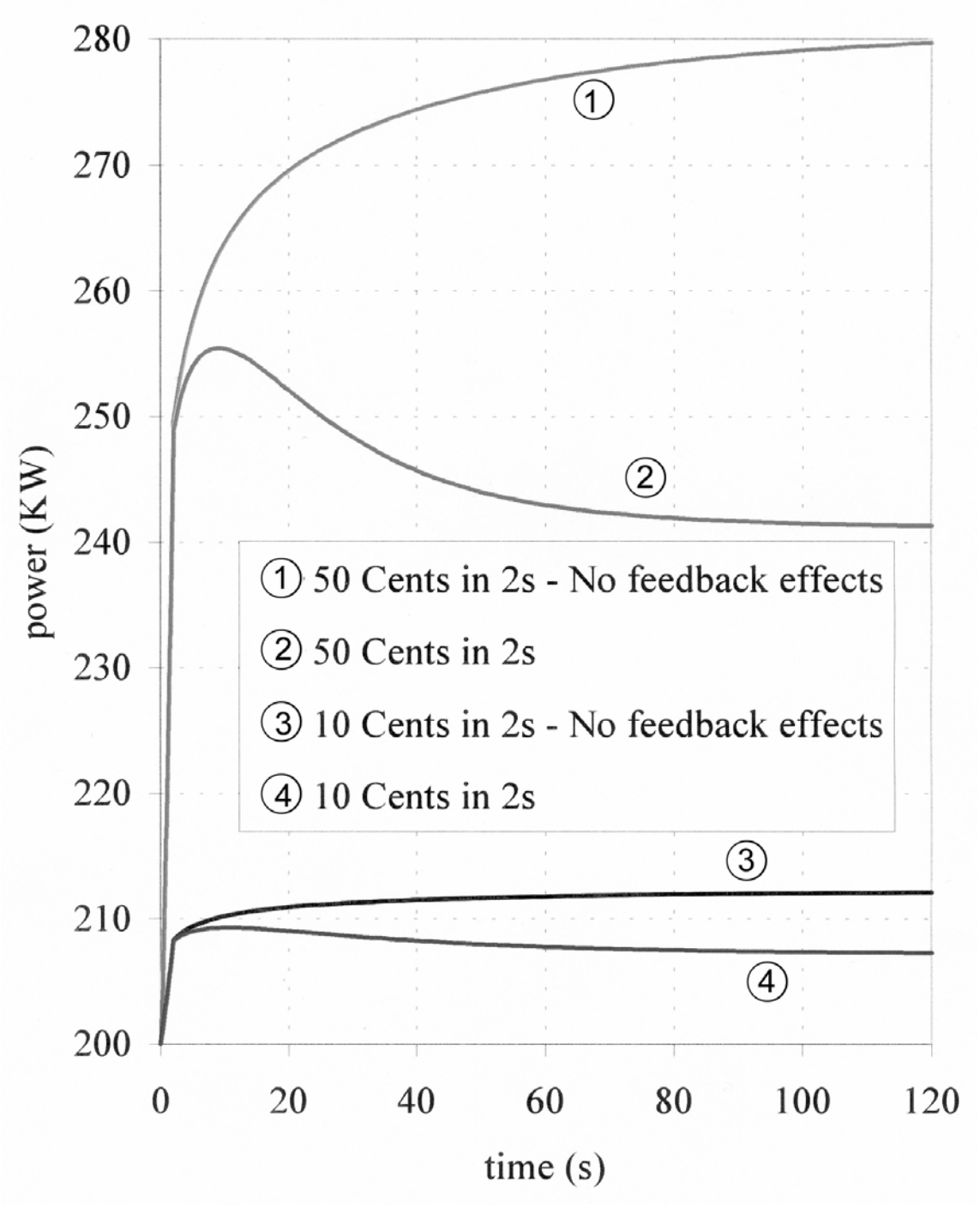

Figure 1 TRADE Reference Configuration (-3.81$) : reactivity insertions from 200 kW

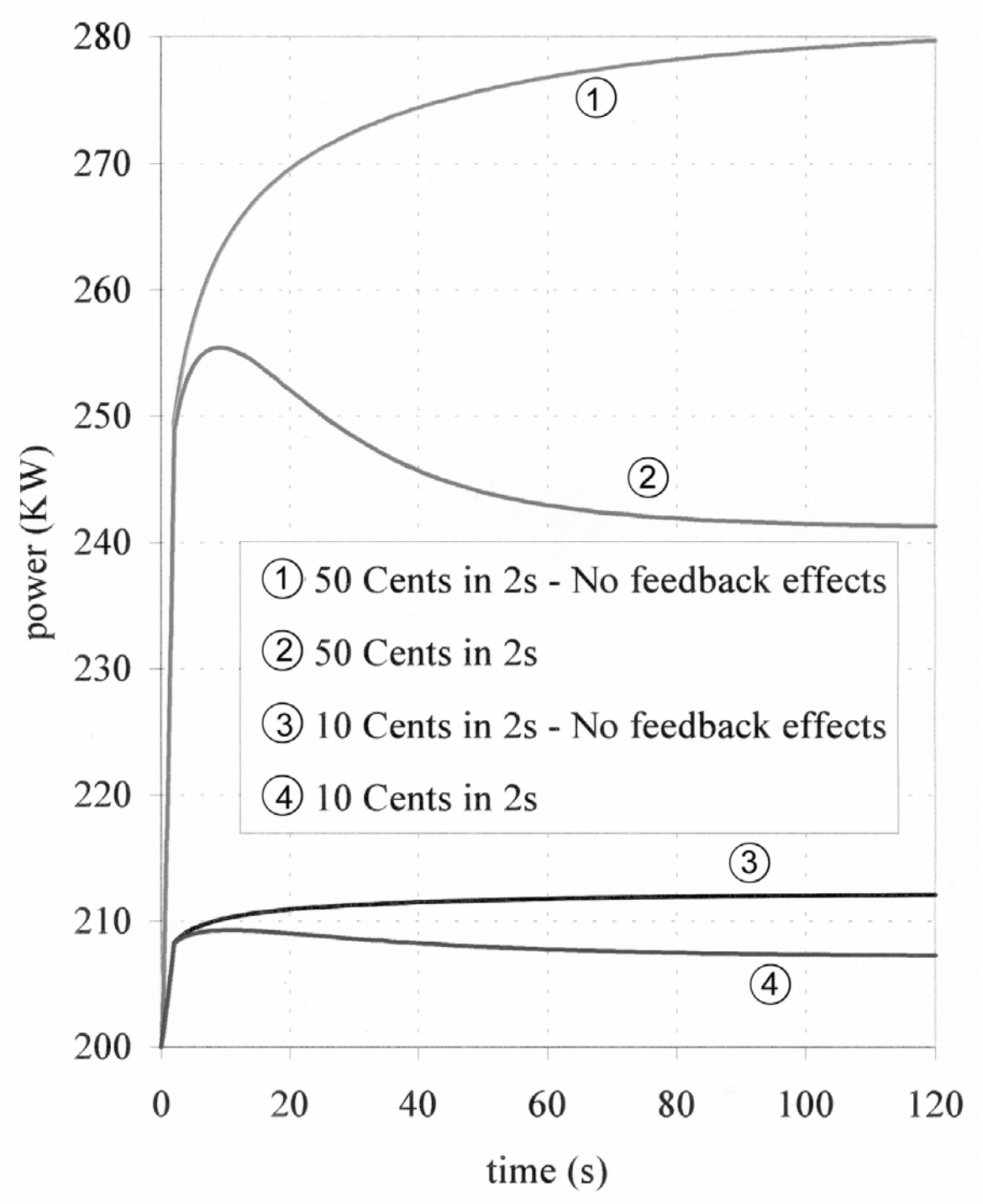

Figure 2 TRADE "High K" Configuration (-1.74$) : reactivity insertions from 200 kW

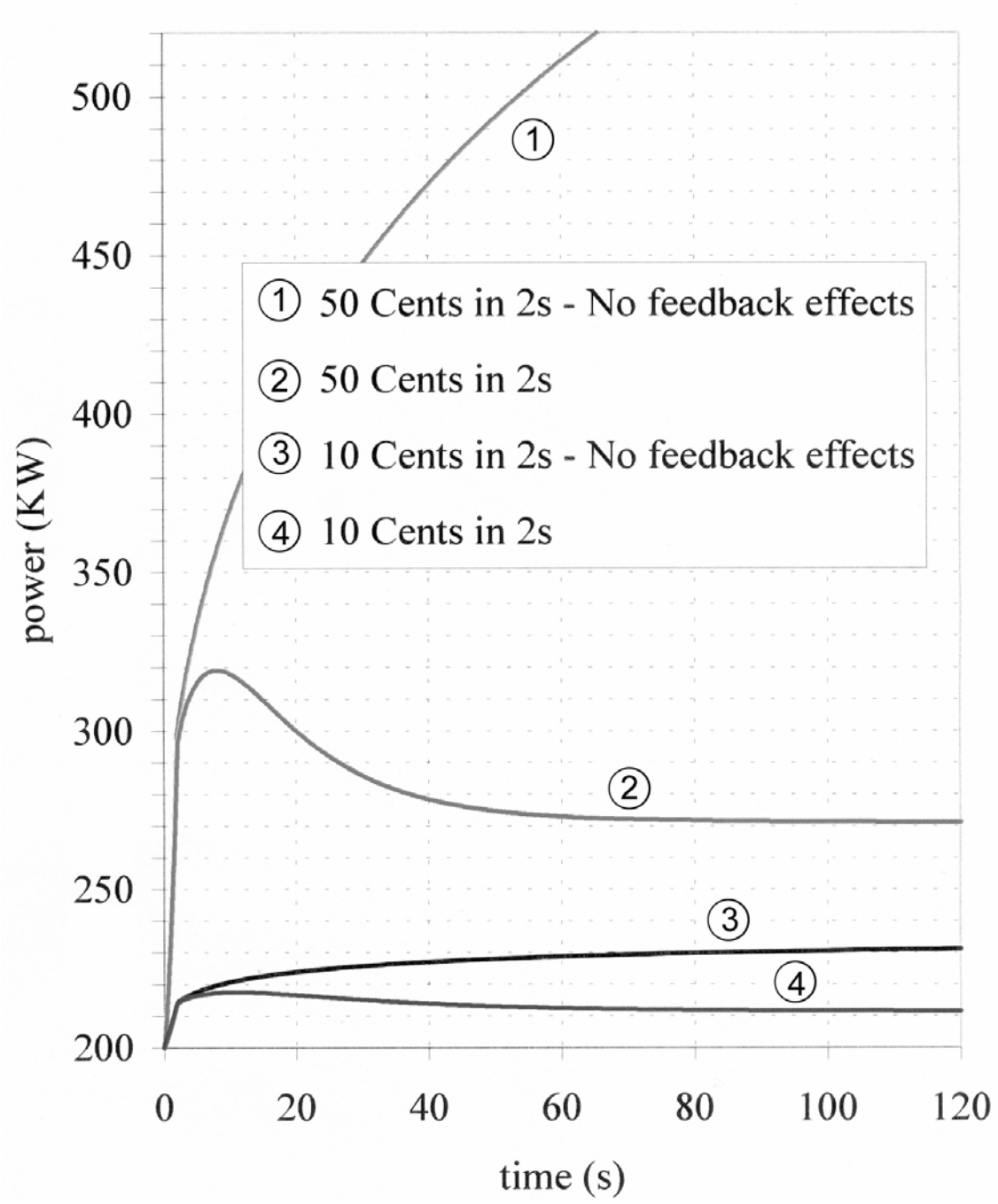

Figure 3 TRADE “Very High K” Config. (-0.72$) : reactivity insertions from 200 kW

Subcriticality = -3.81$

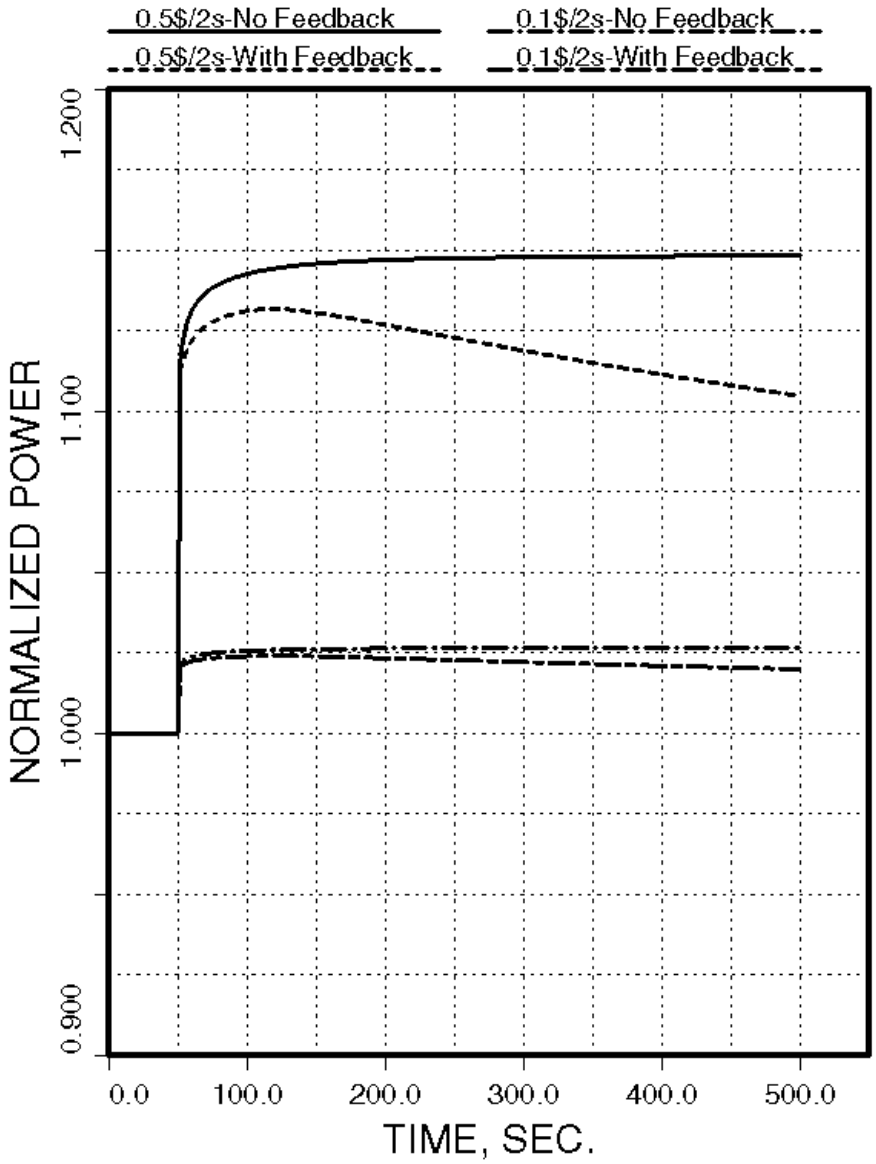

Figure 4 Power transient in a 'real' Na cooled ADS corresponding to the figure 2 for TRADE (calculated)

Subcriticality = -1.74$

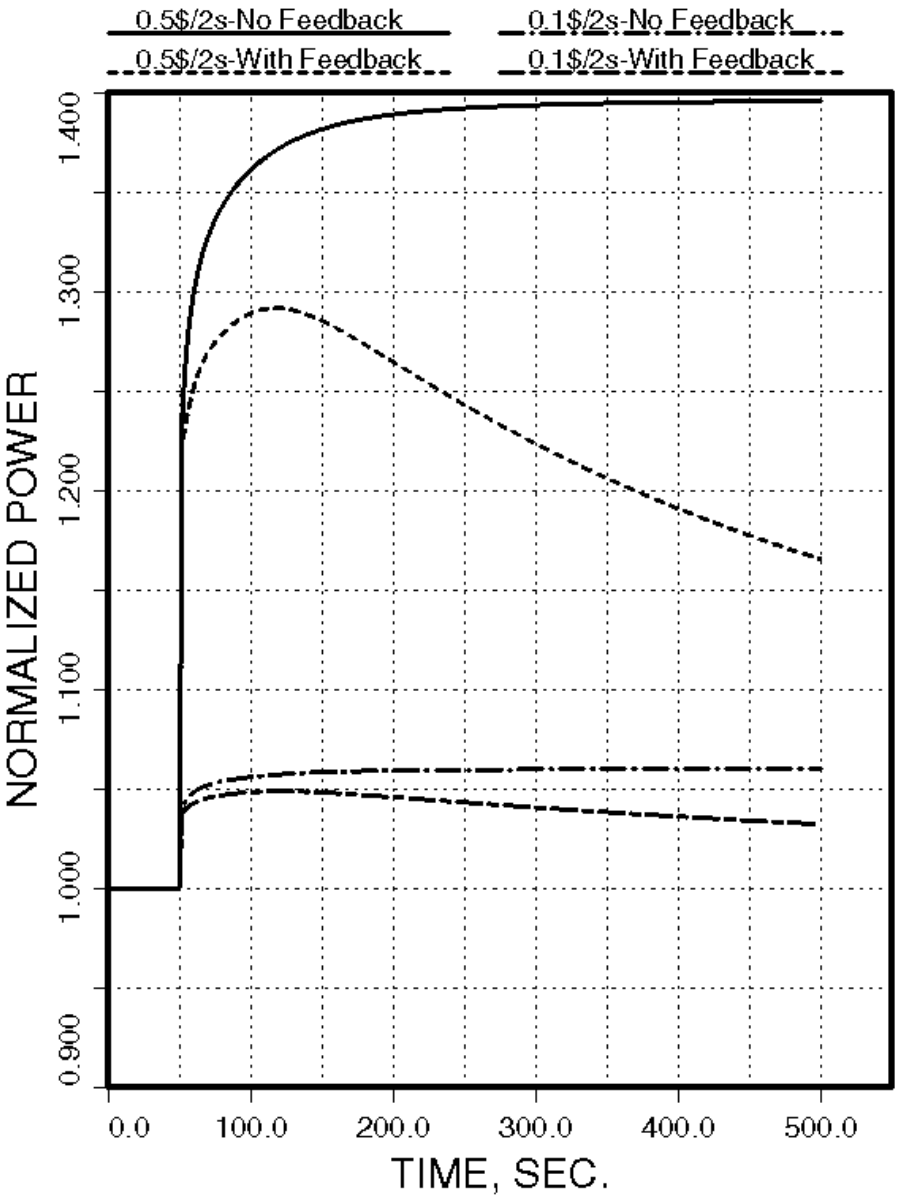

Figure 5 Power transient in a 'real' Na cooled ADS corresponding to the figure 3 for TRADE (calculated)

Subcriticality = -0.72$

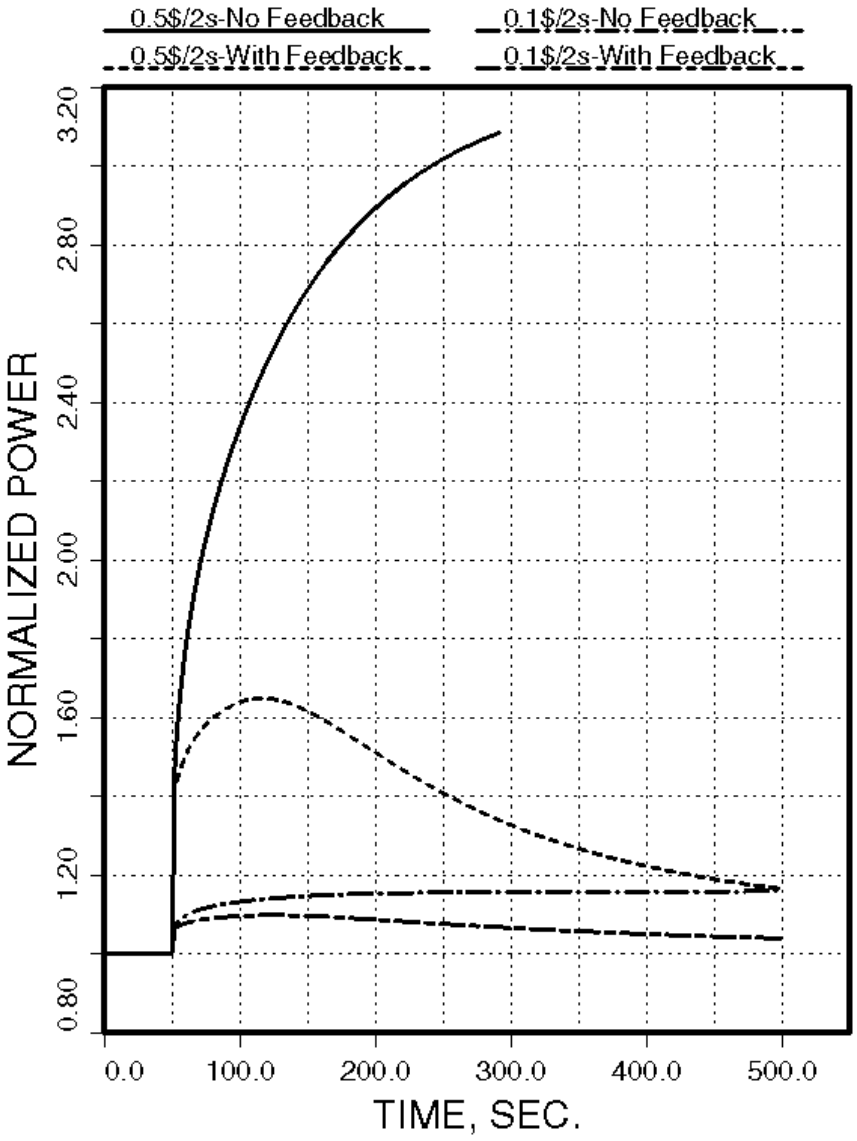

Figure 6 Power transient in a 'real' Na cooled ADS corresponding to the figure 4 for TRADE (calculated)

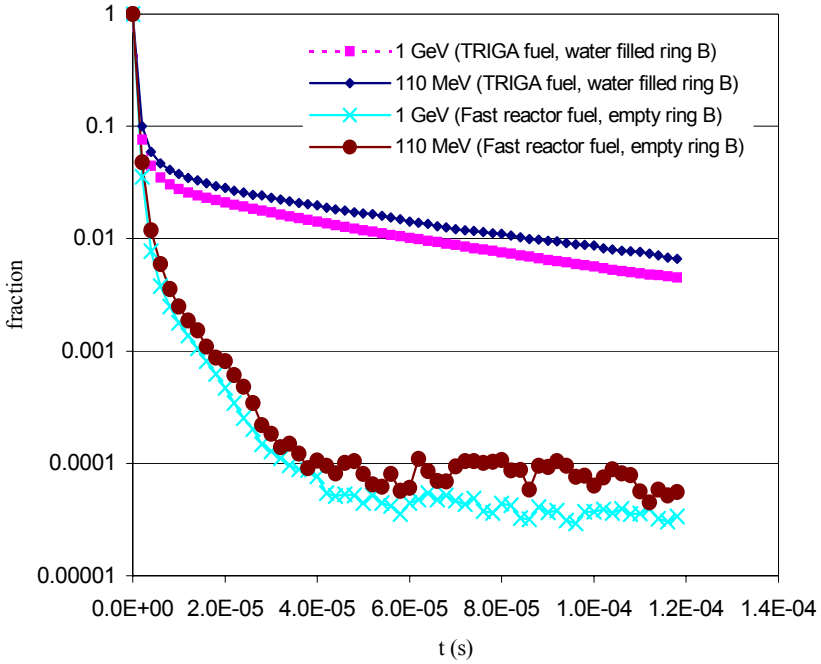

Figure 7 Evolution of the Spallation Neutron Flux as Function of Energy and Fuel Type. Ring B is filled with water or empty.

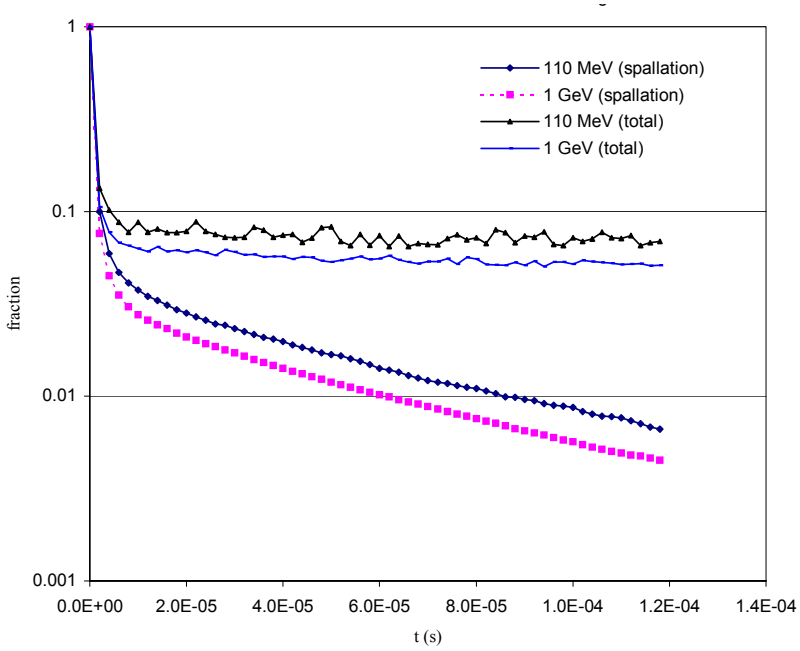

Figure 8 Evolution of the Neutron Flux as Function of Time in the TRIGA Fuel. Ring B is filled with water.

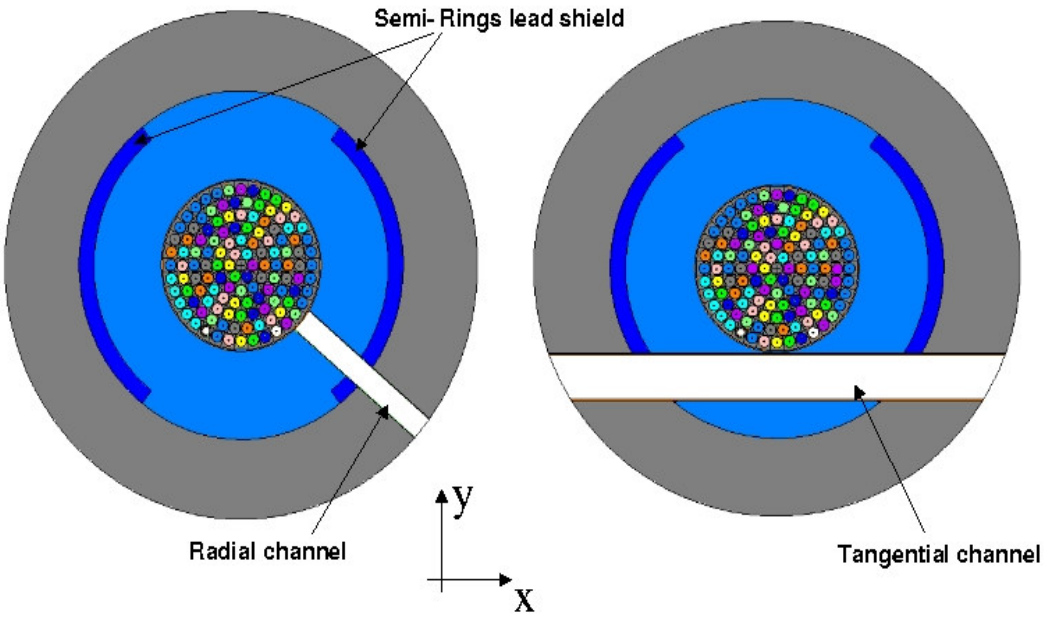

Figure 9 TRIGA core

Figure 10 TRIGA fuel rod

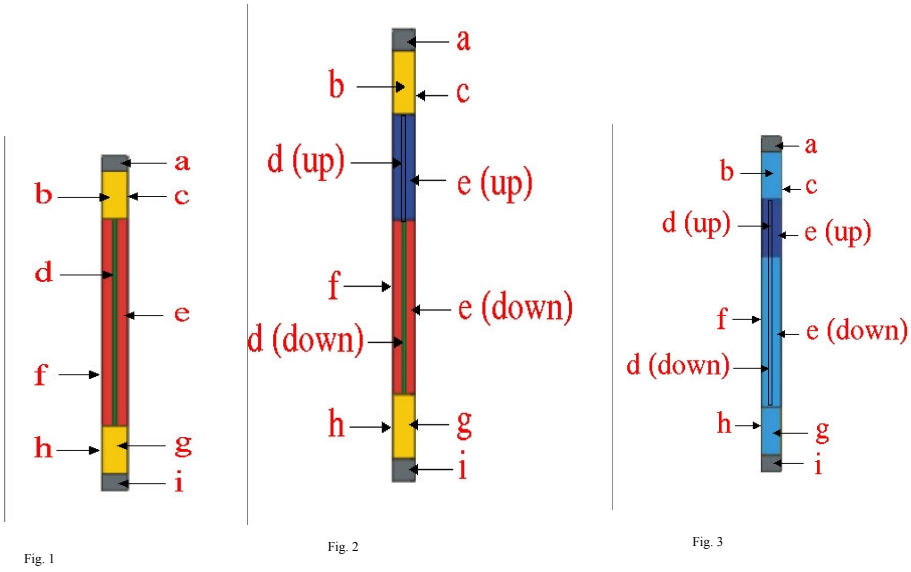

Figure 11 TRIGA fuel and control rods partitioning

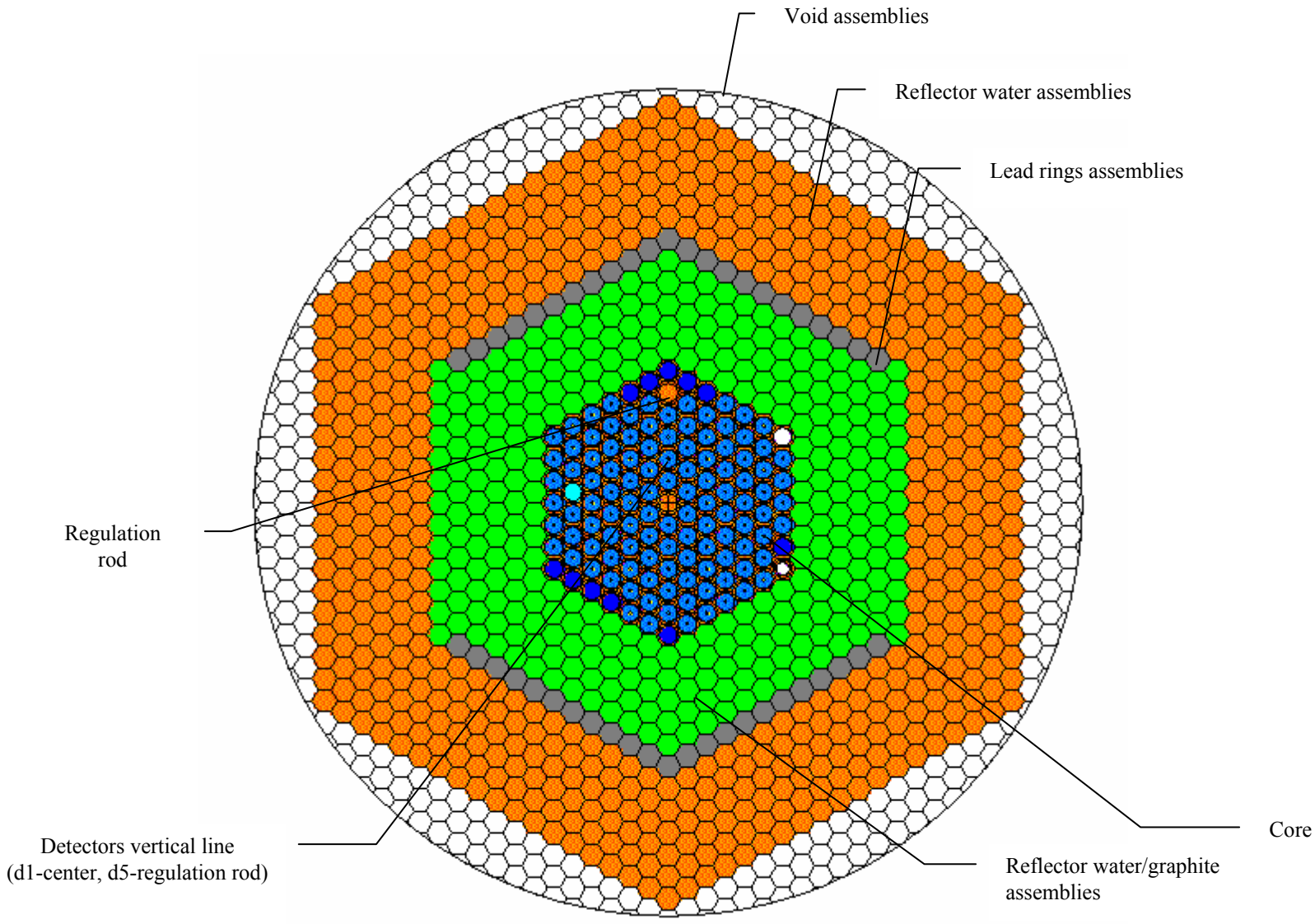

Figure 12 Hexagonal model of TRIGA reactor

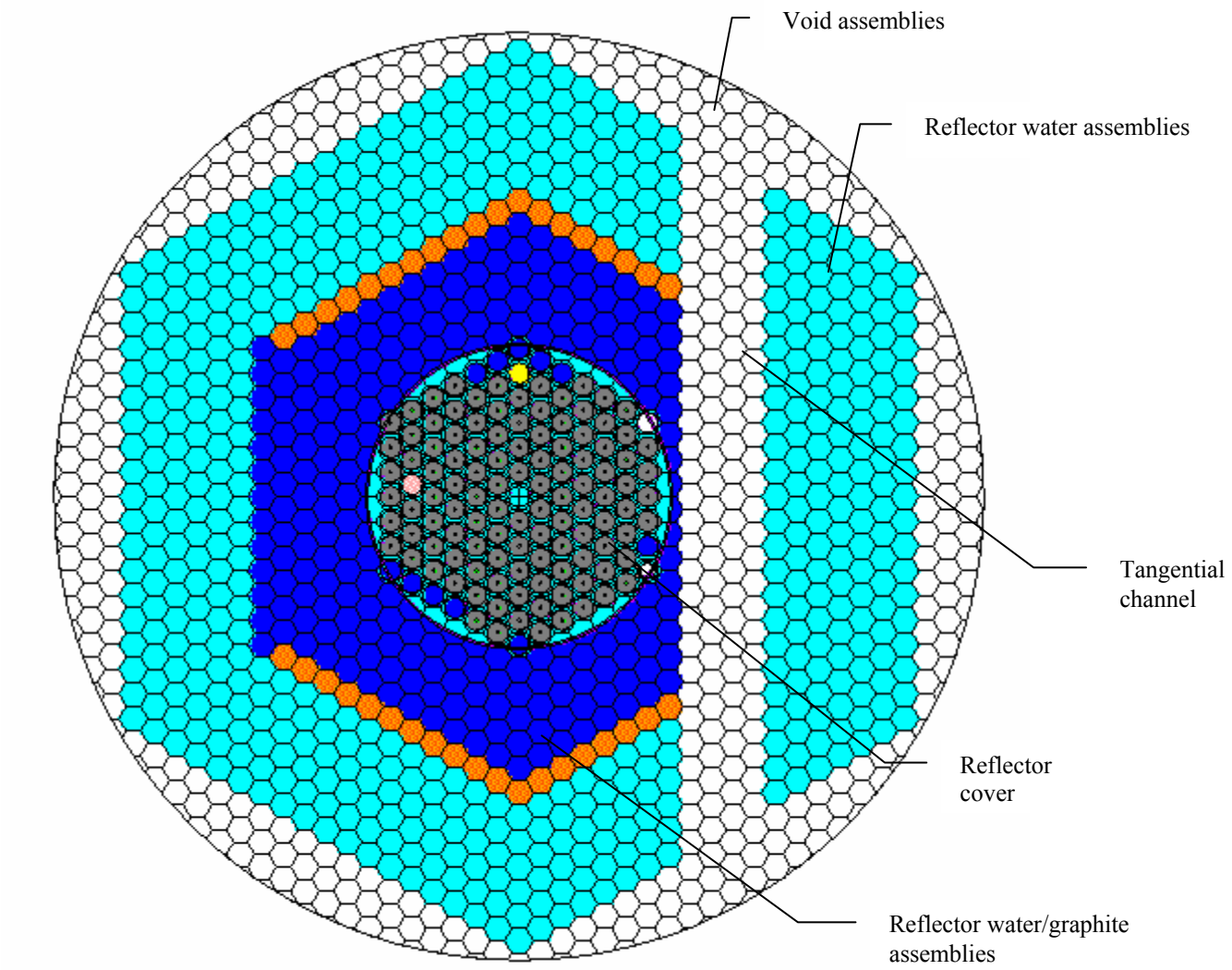

Figure 13 Hexagonal model of TRIGA reactor with tangential and radial channels and the reflector cover.

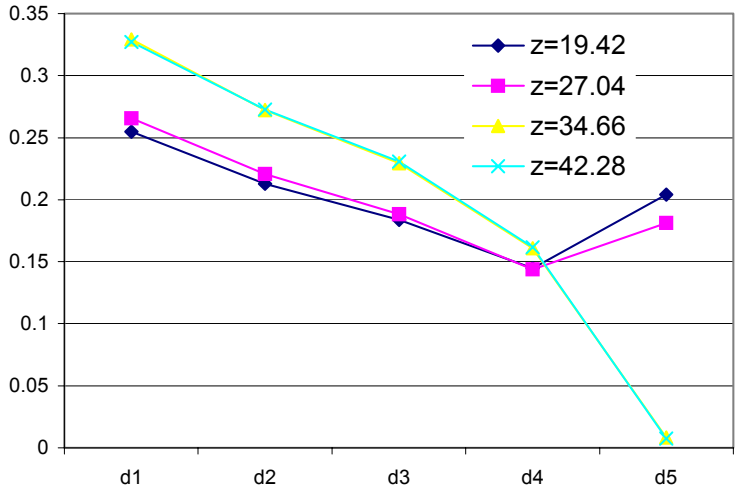

Figure 14 Reaction rates distribution calculated with VARIANT option in DIF3D.

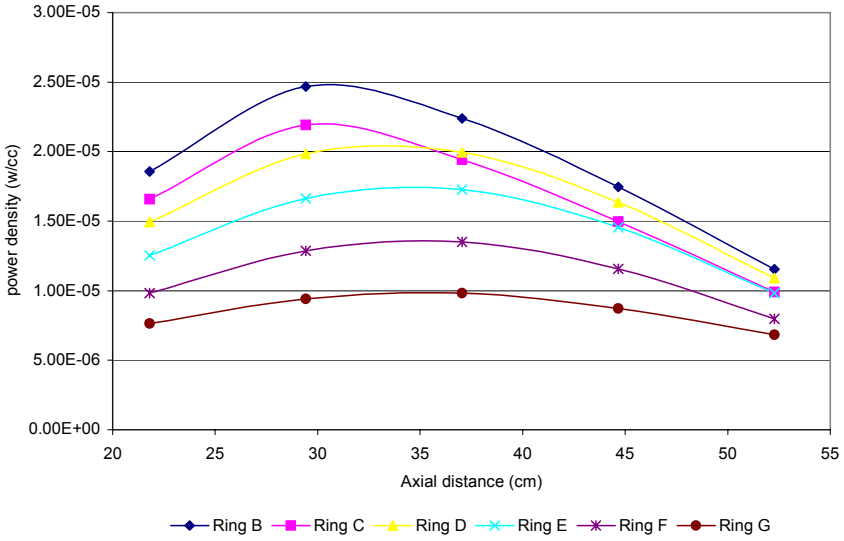

Figure 15 Axial power density profile

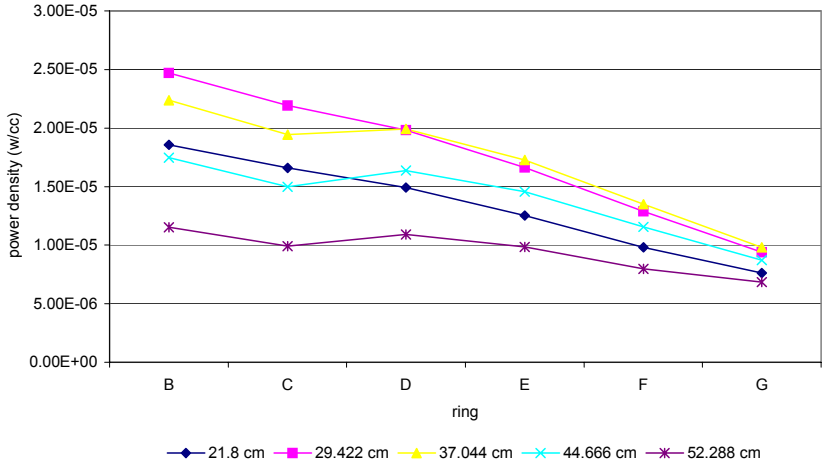

Figure 16 Radial power density profile

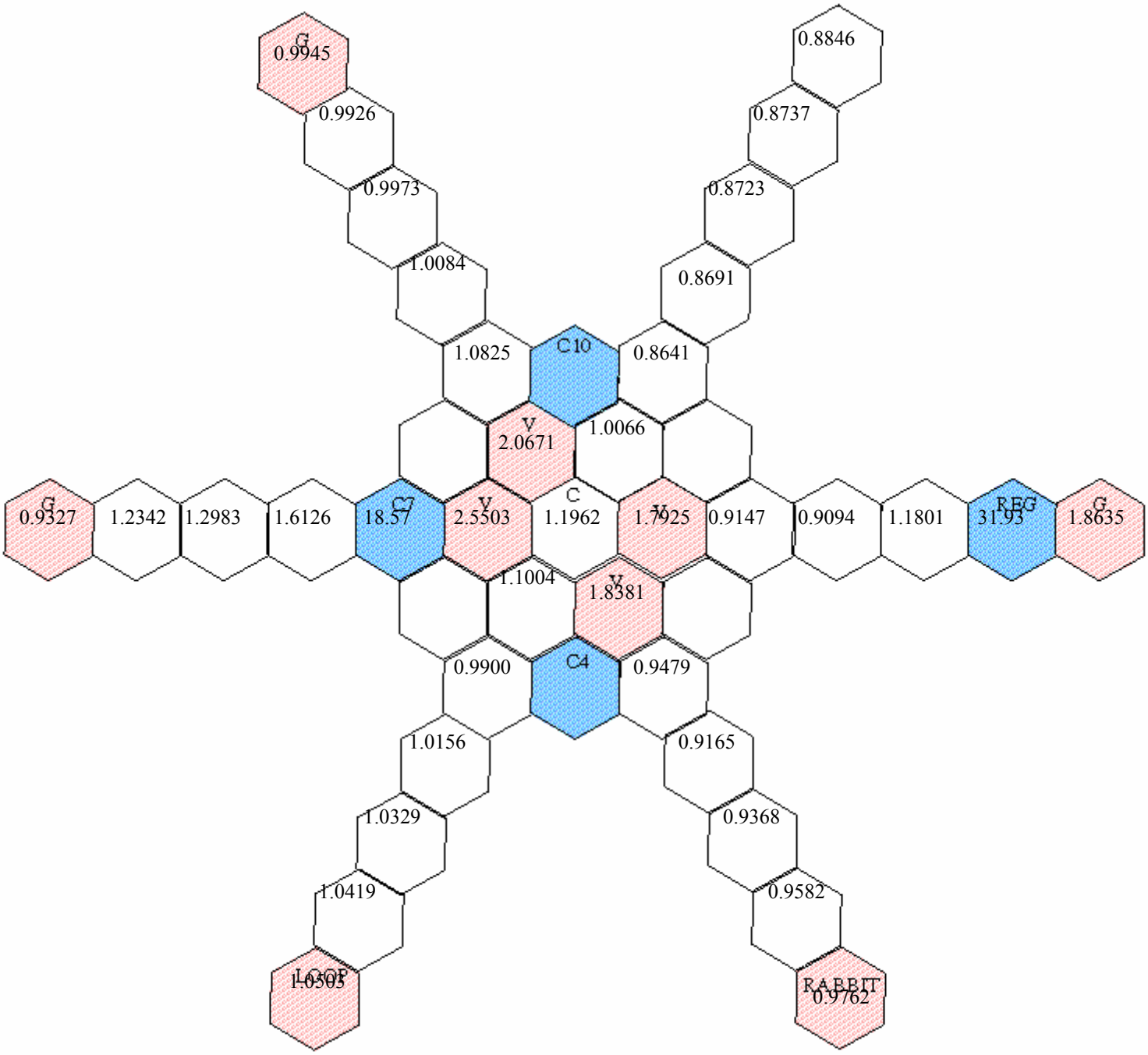

Figure 17 MSM factors. Radial traverses for the critical configuration 1 (critical configuration 4 is taken as a reference). All white hexagons are fuel filled. Control rods are C4 (SEC), C7 (SH2) and C10 (SH1). Graphite elements are denoted G. The voided assemblies (with diluted water as described in the text) are denoted V.

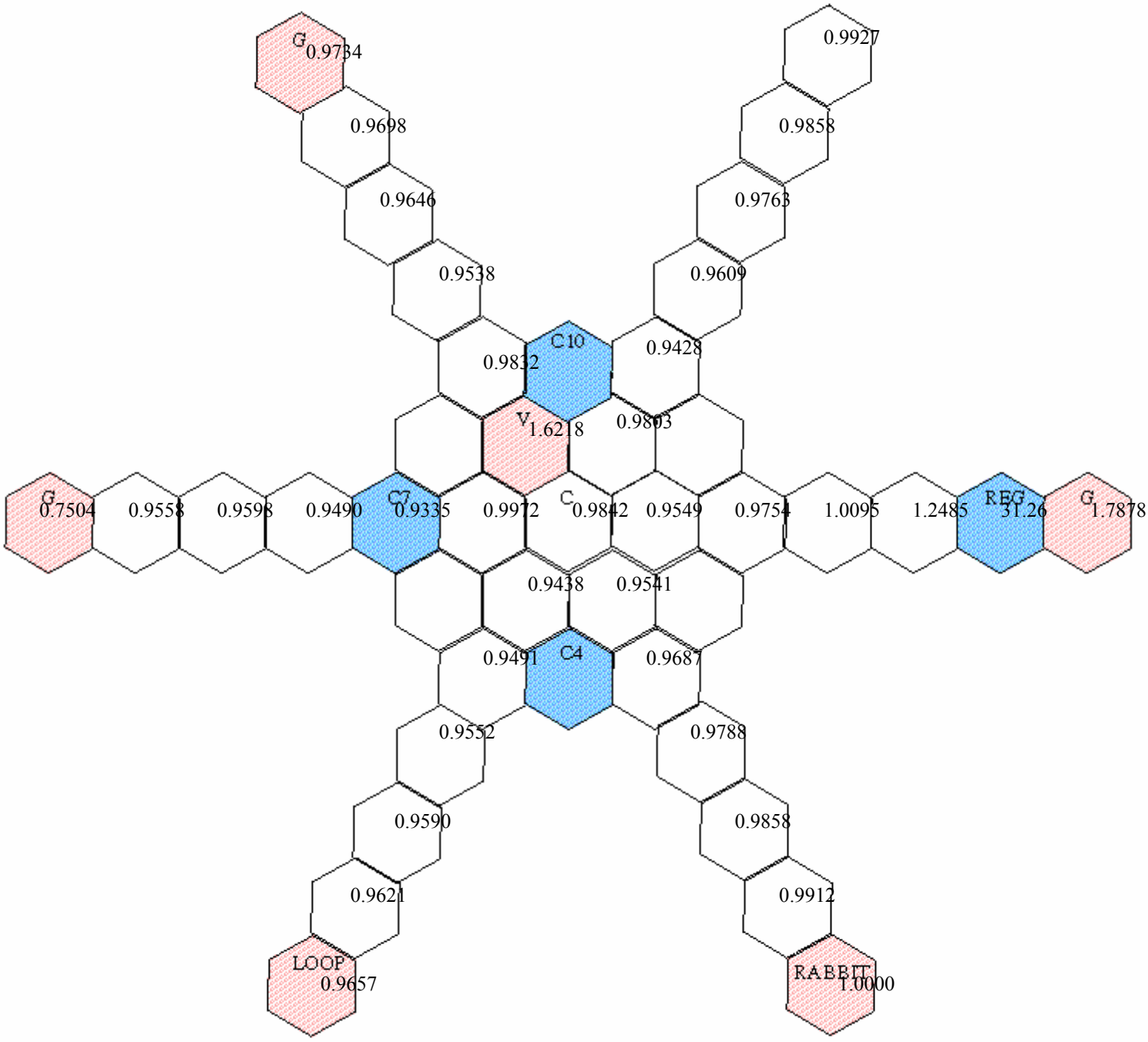

Figure 18 MSM factors. Radial traverses for the critical configuration 2 (critical configuration 4 is taken as a reference). All white hexagons are fuel filled. Control rods are C4 (SEC), C7 (SH2) and C10 (SH1). Graphite elements are denoted G. The voided assemblies (with diluted water as described in the text) are denoted V.

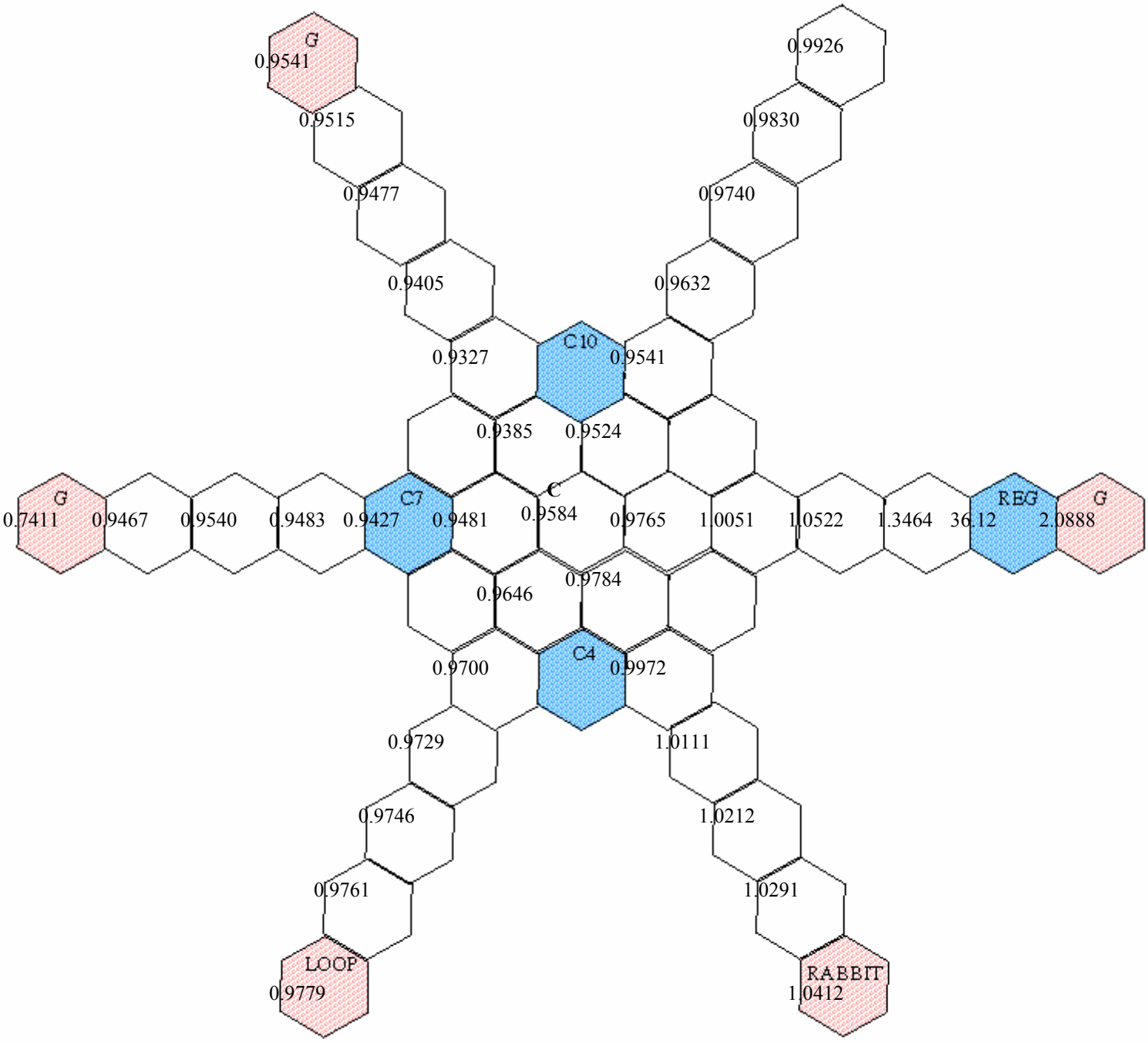

Figure 19 MSM factors. Radial traverses for the critical configuration 3 (critical configuration 4 is taken as a reference). All white hexagons are fuel filled. Control rods are C4 (SEC), C7 (SH2) and C10 (SH1). Graphite elements are denoted G.

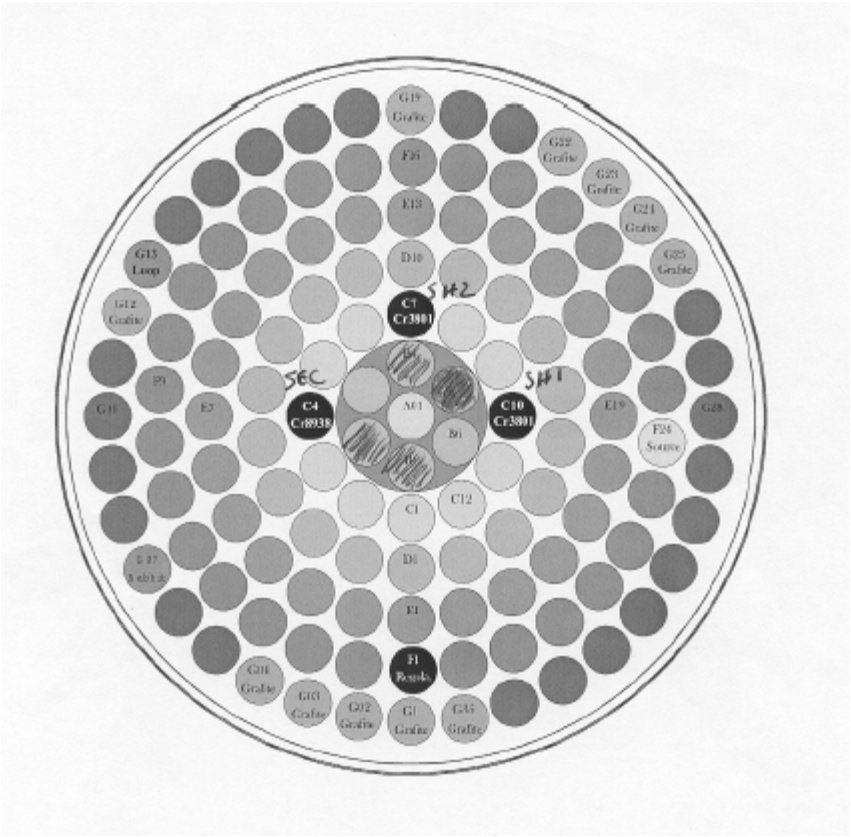

Figure 20 Core map

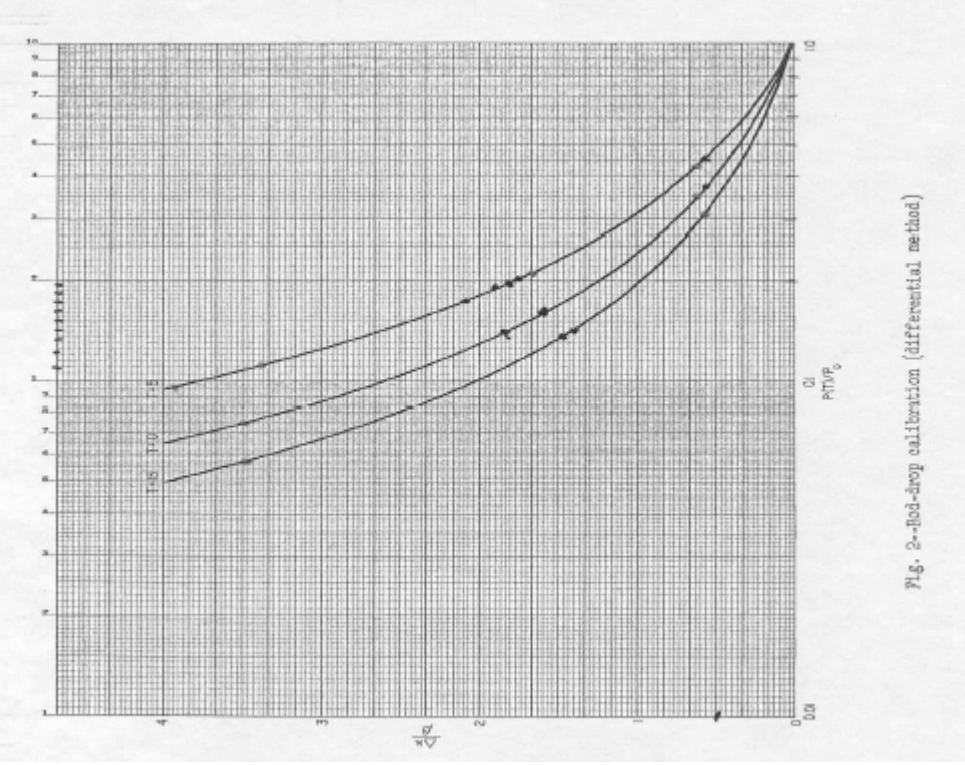

Figure 21 Rod drop data from GA

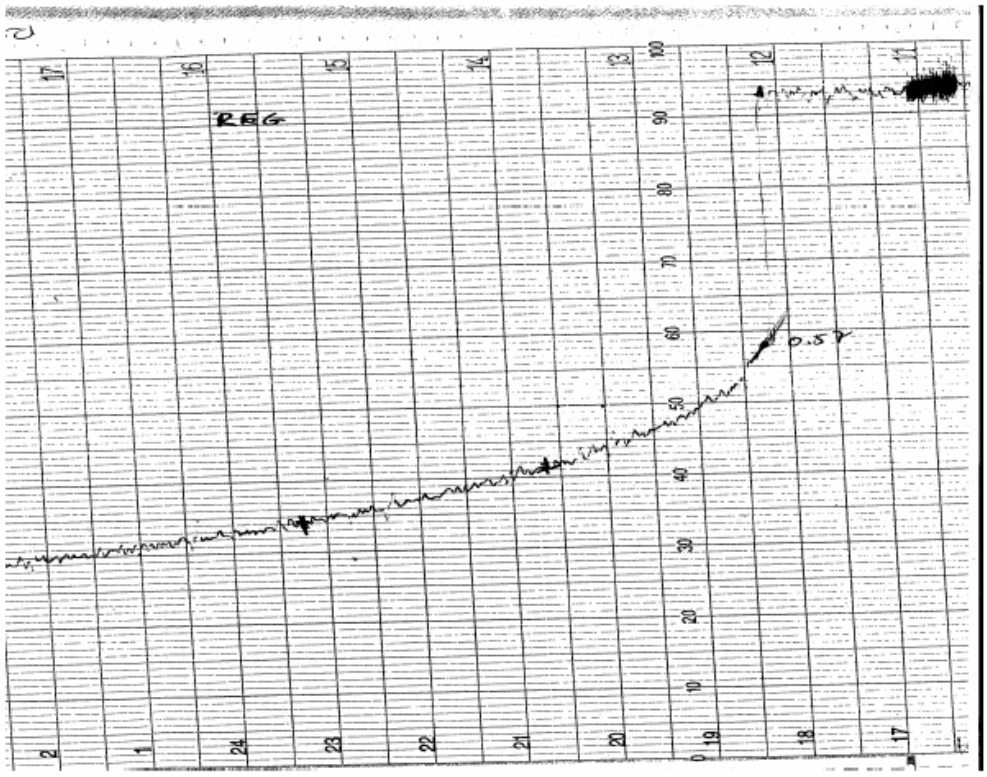

Figure 22 Regulation rod drop

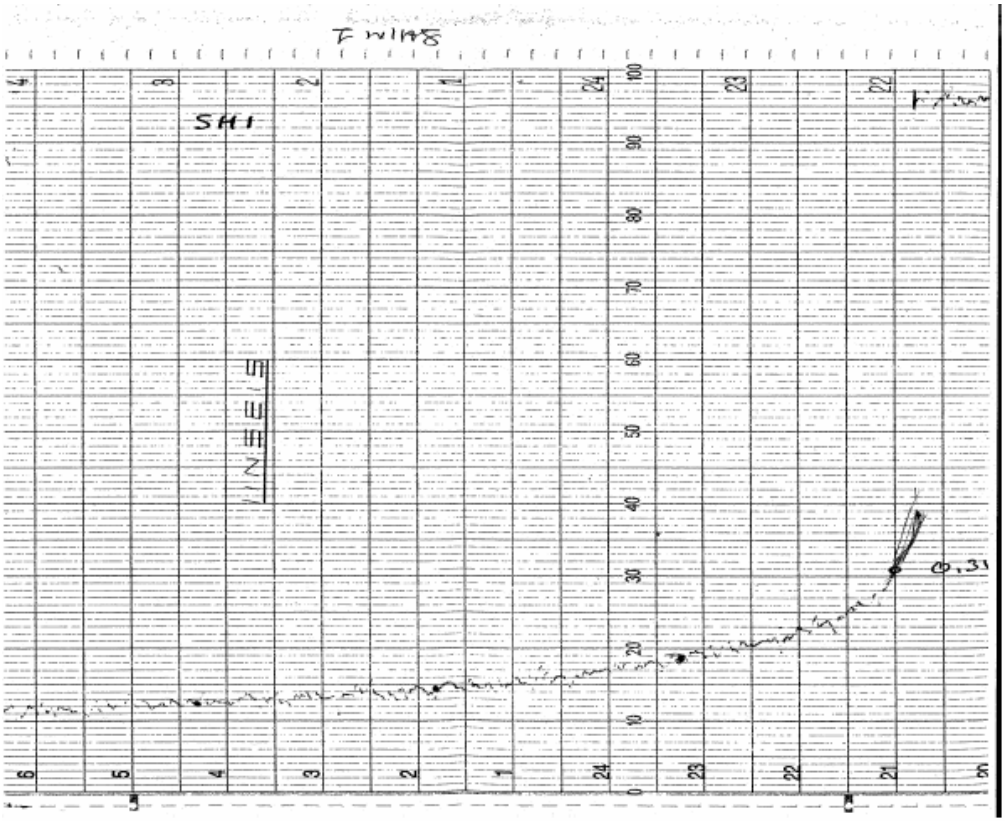

Figure 23 Shim 1 drop

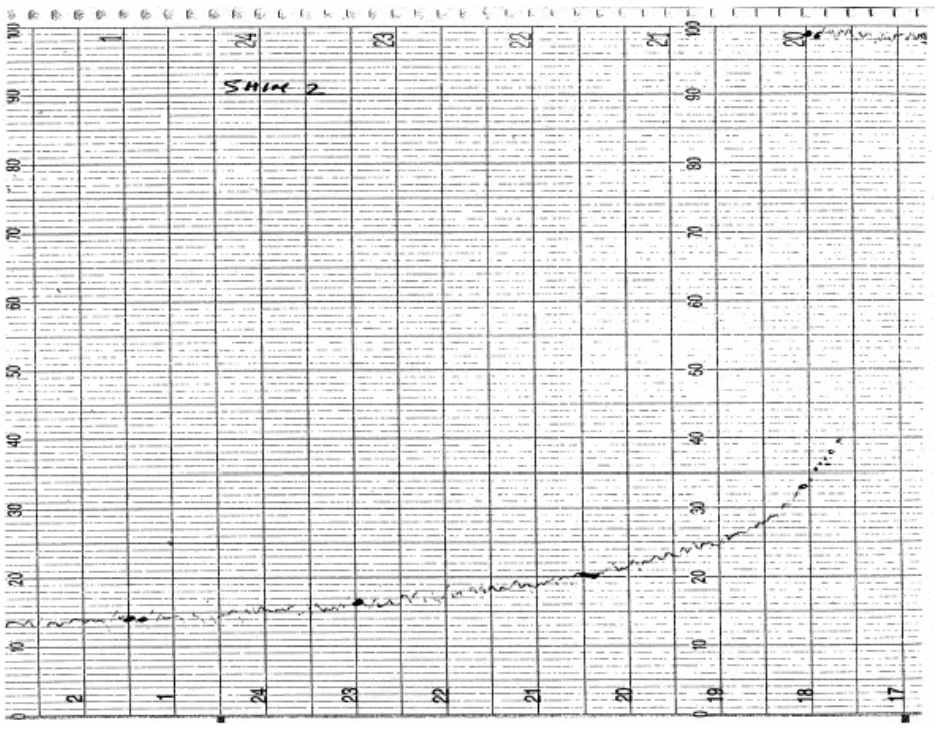

Figure 24 Shim 2 drop

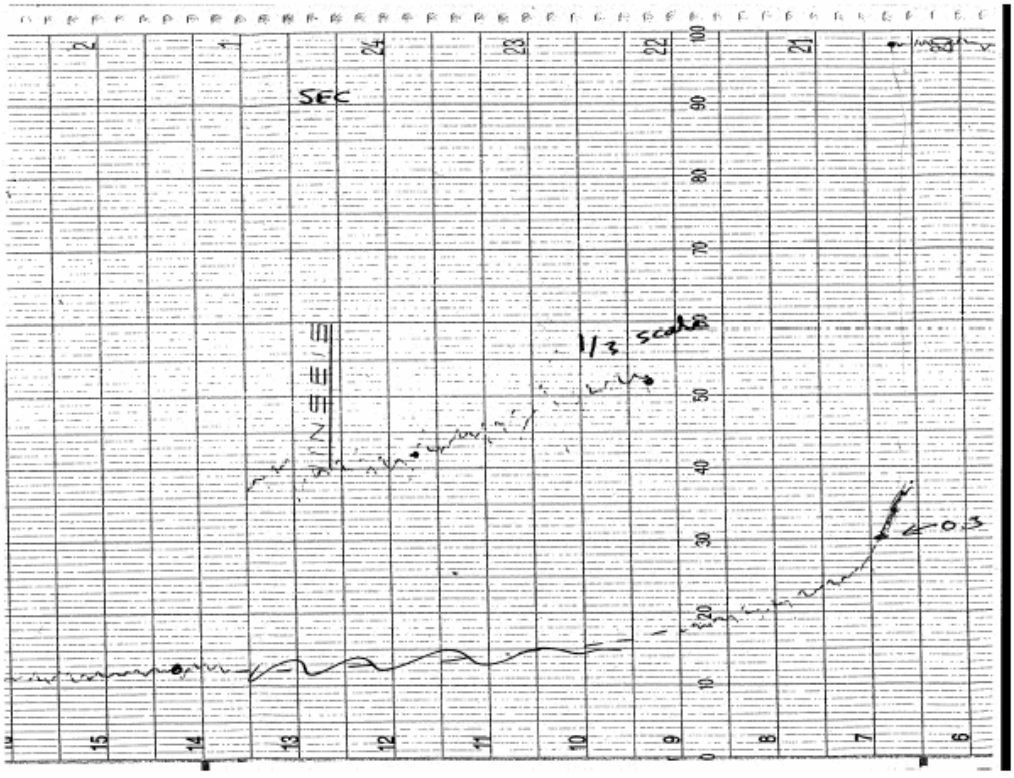

Figure 25 Security rod drop

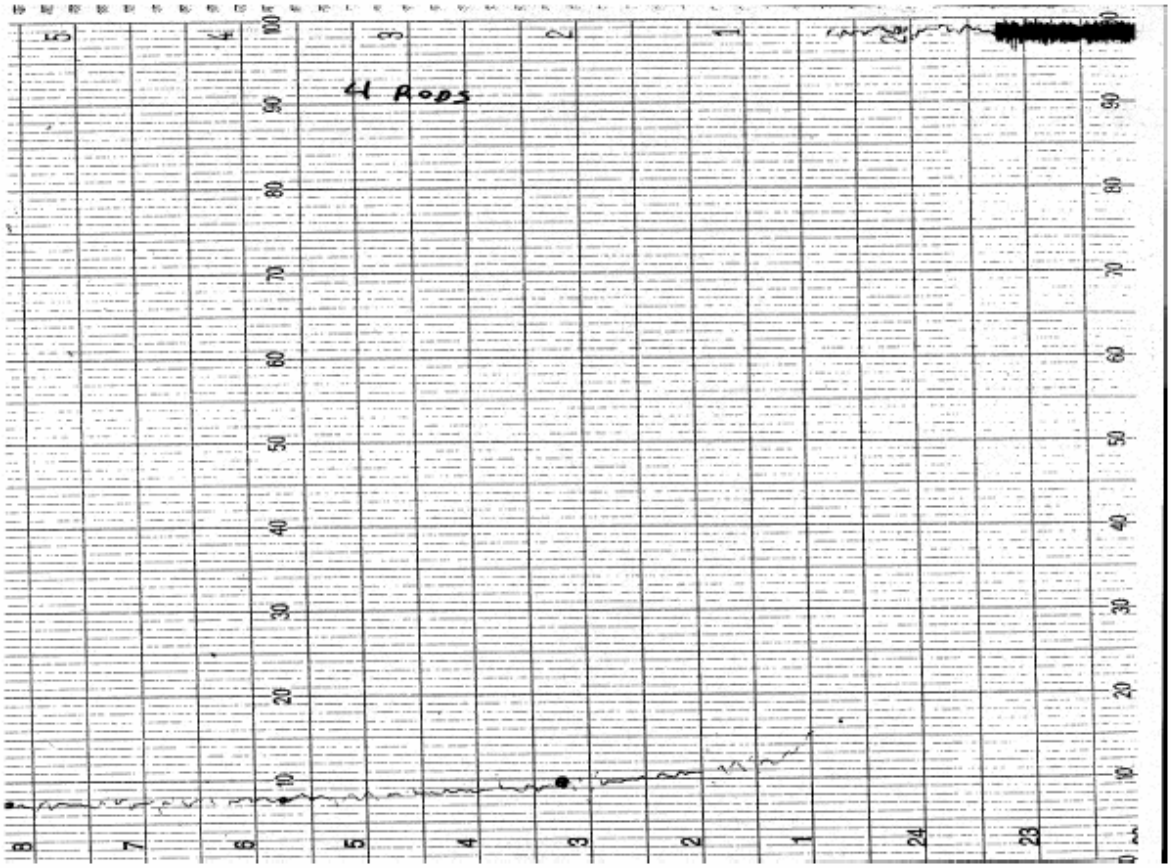

Figure 26 All rods drop

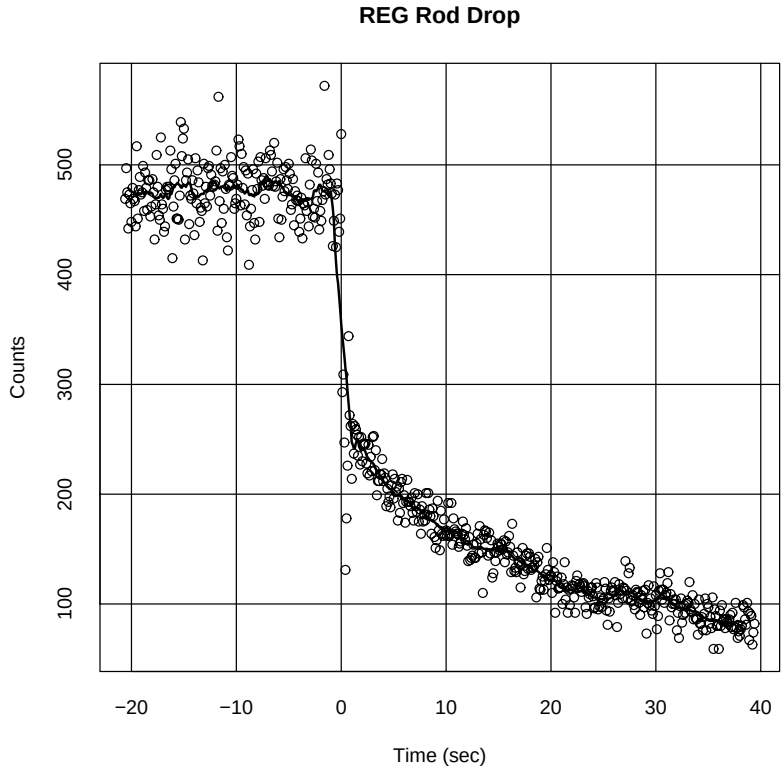

Figure 27 Regulation rod drop

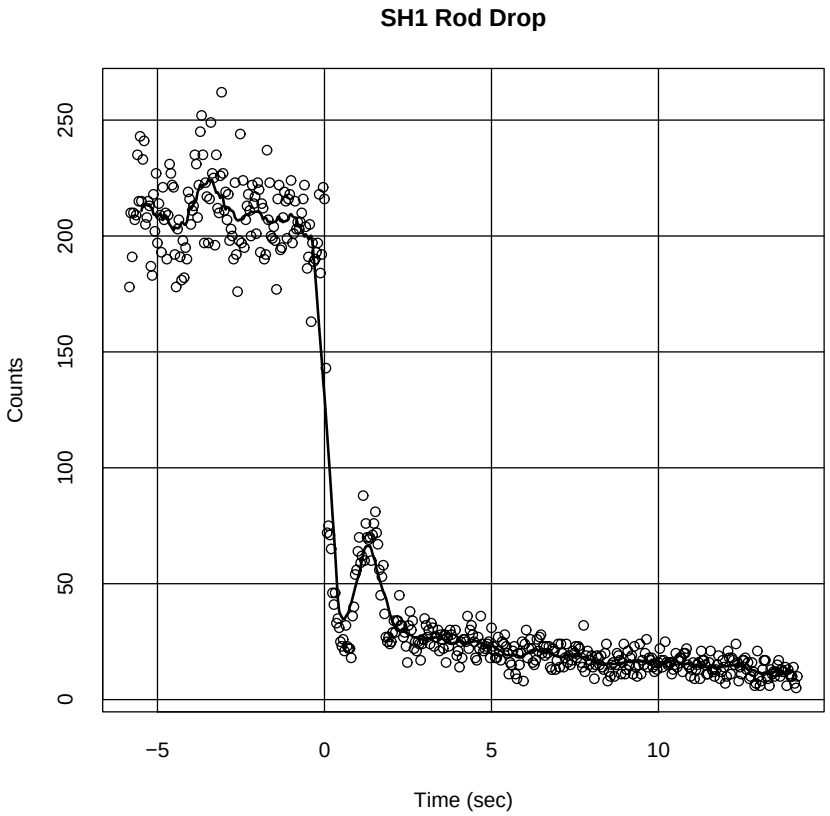

Figure 28 SH1 drop

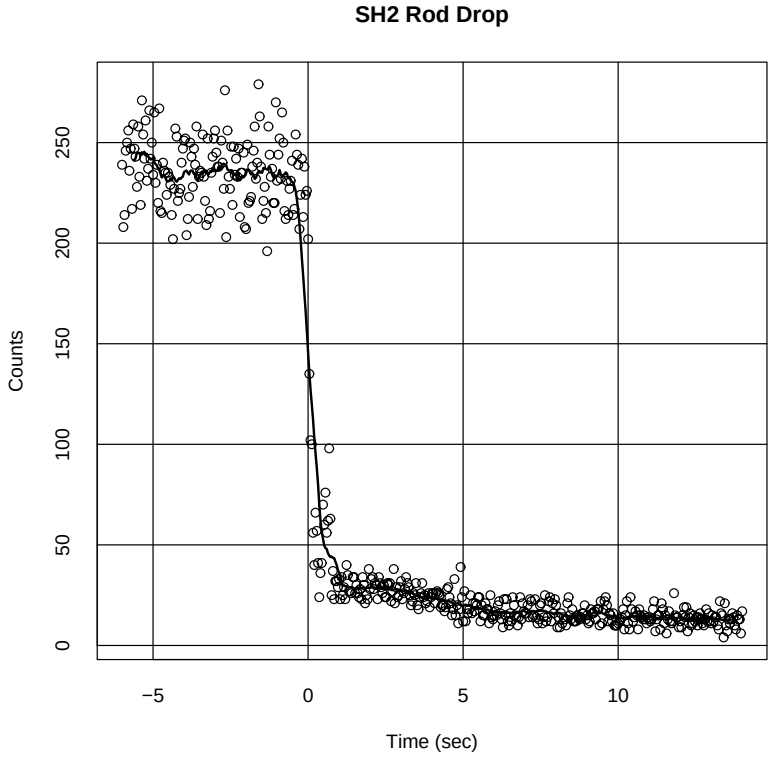

Figure 29 SH 2 drop

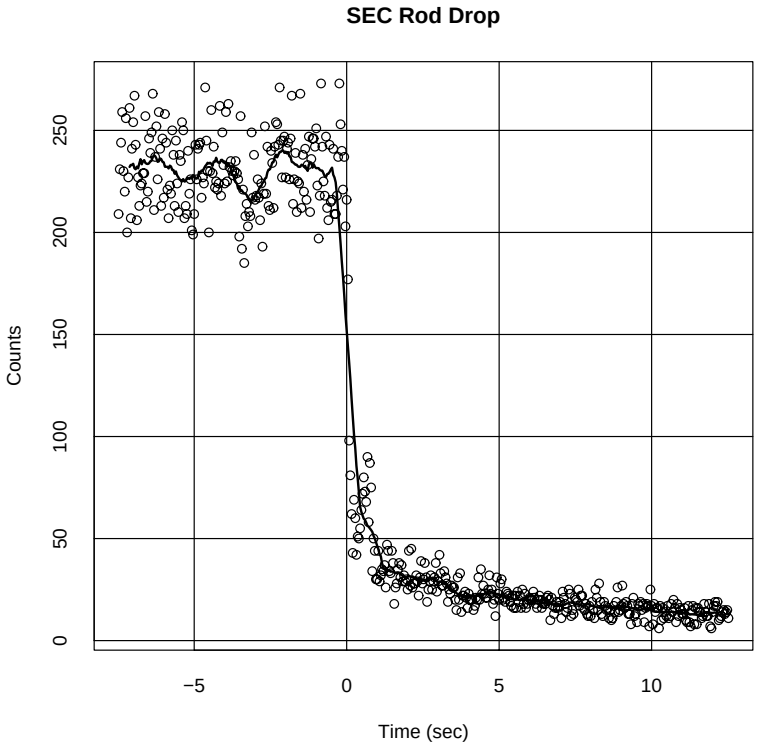

Figure 30 Security rod drop

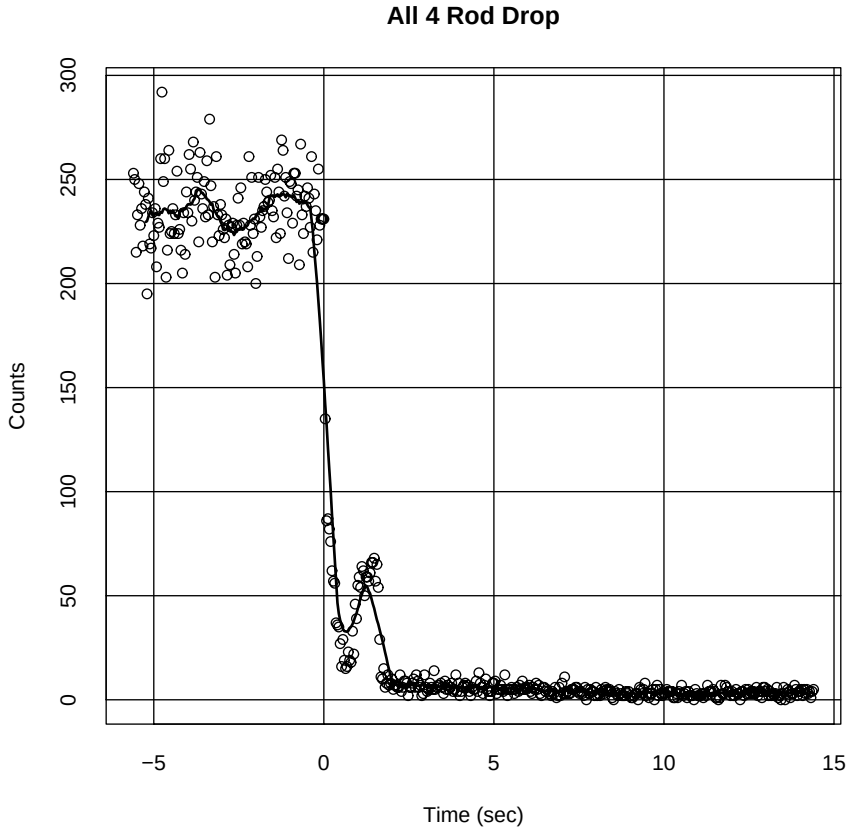

Figure 31 All rods drop

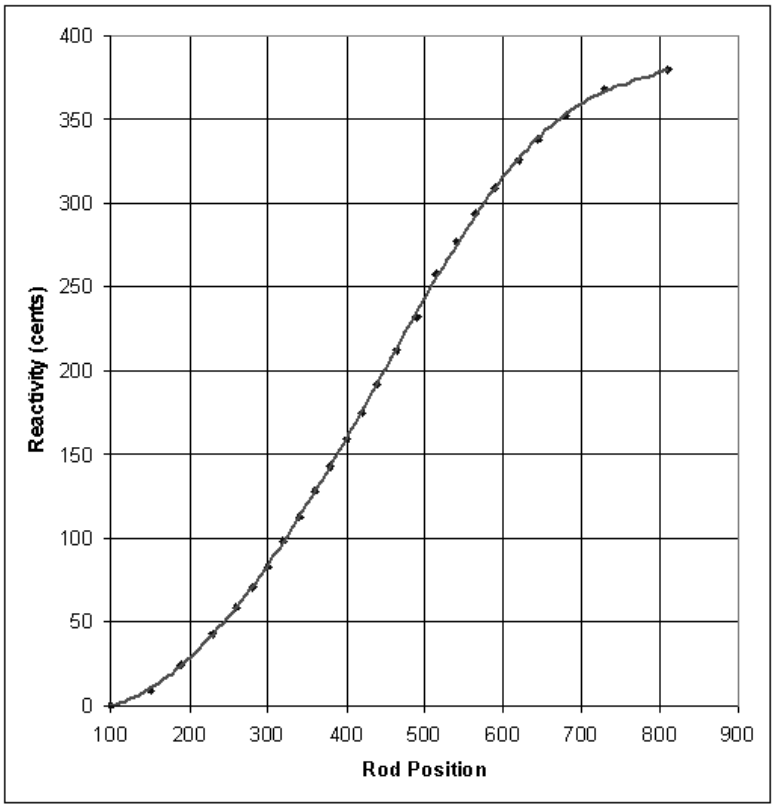

Figure 32 Safety rod. Total 379.51 cents

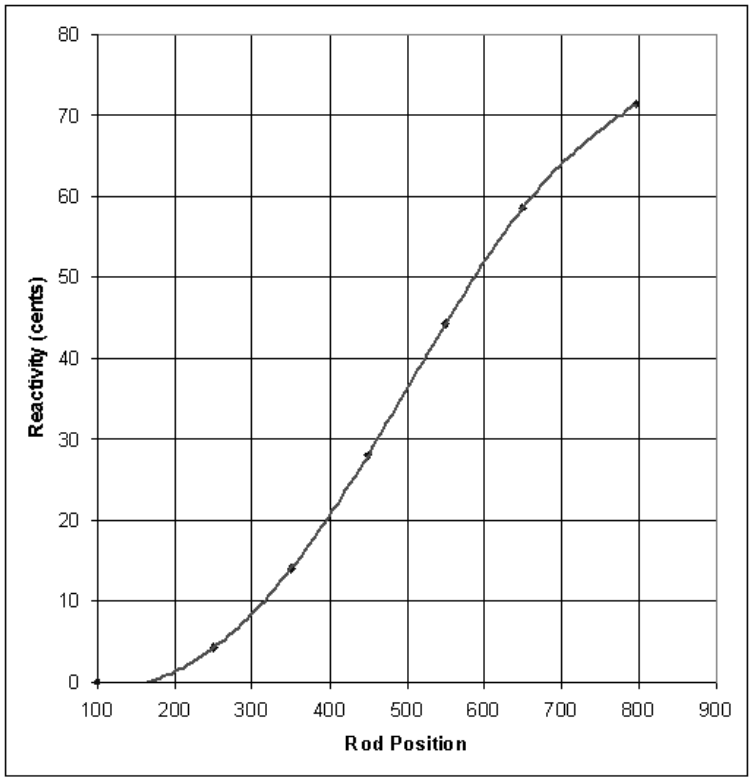

Figure 33 Regulation rod. Total 71.39 cents

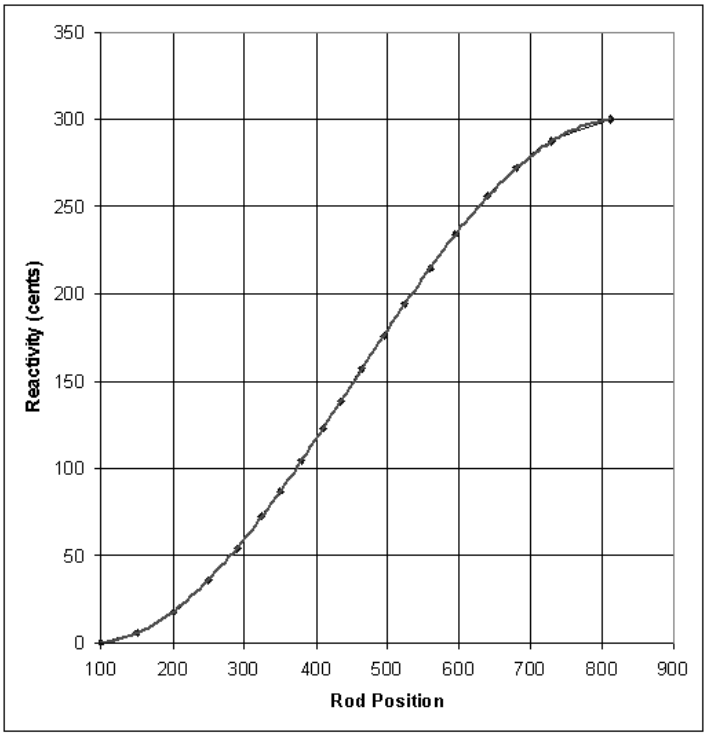

Figure 34 SHIM1. Total 300.27 cents

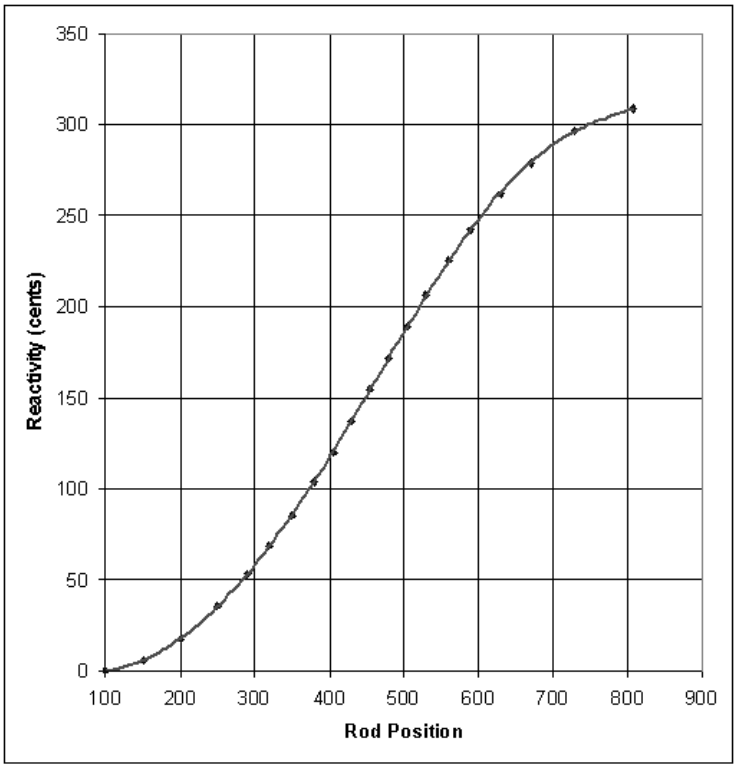

Figure 35 SHIM2. Total 308.49 cents

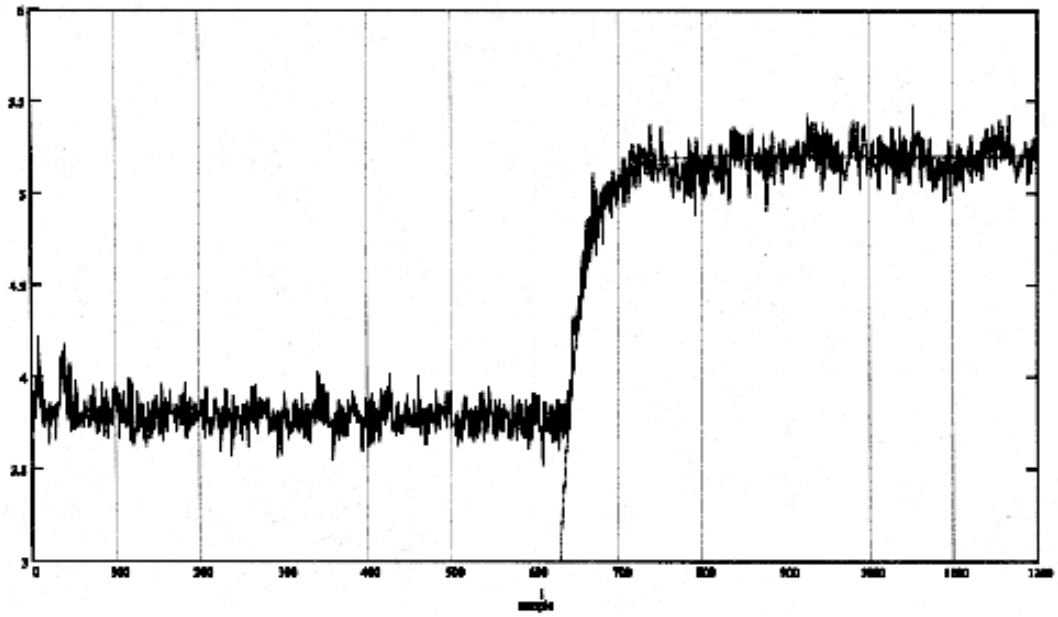

Figure 36 Power transient with temperature coefficient effect

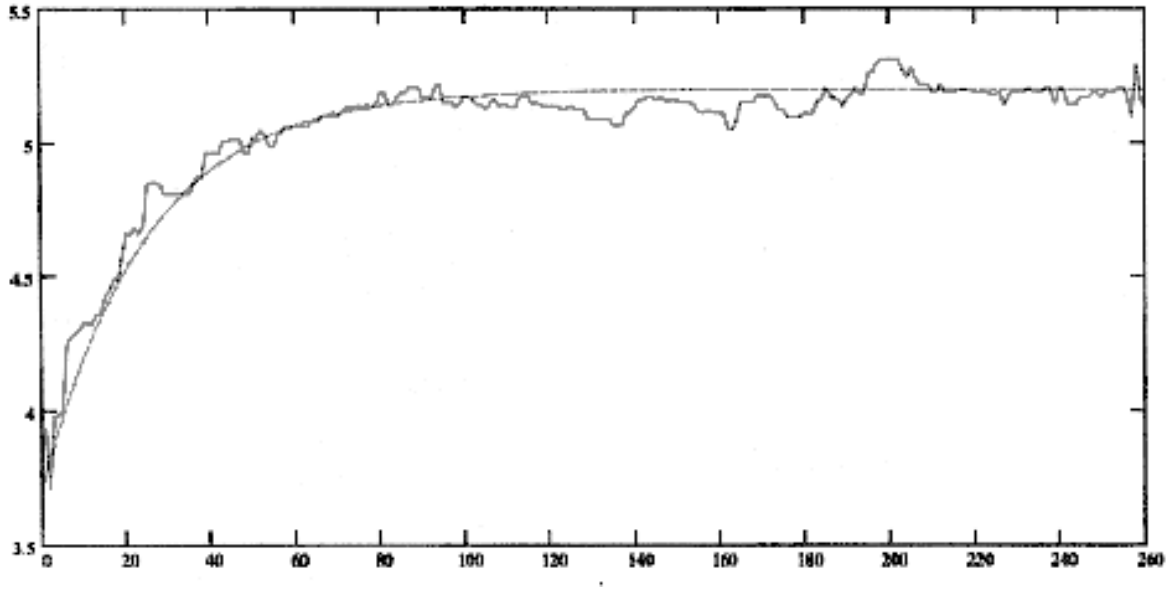

Figure 37 Total energy of transients

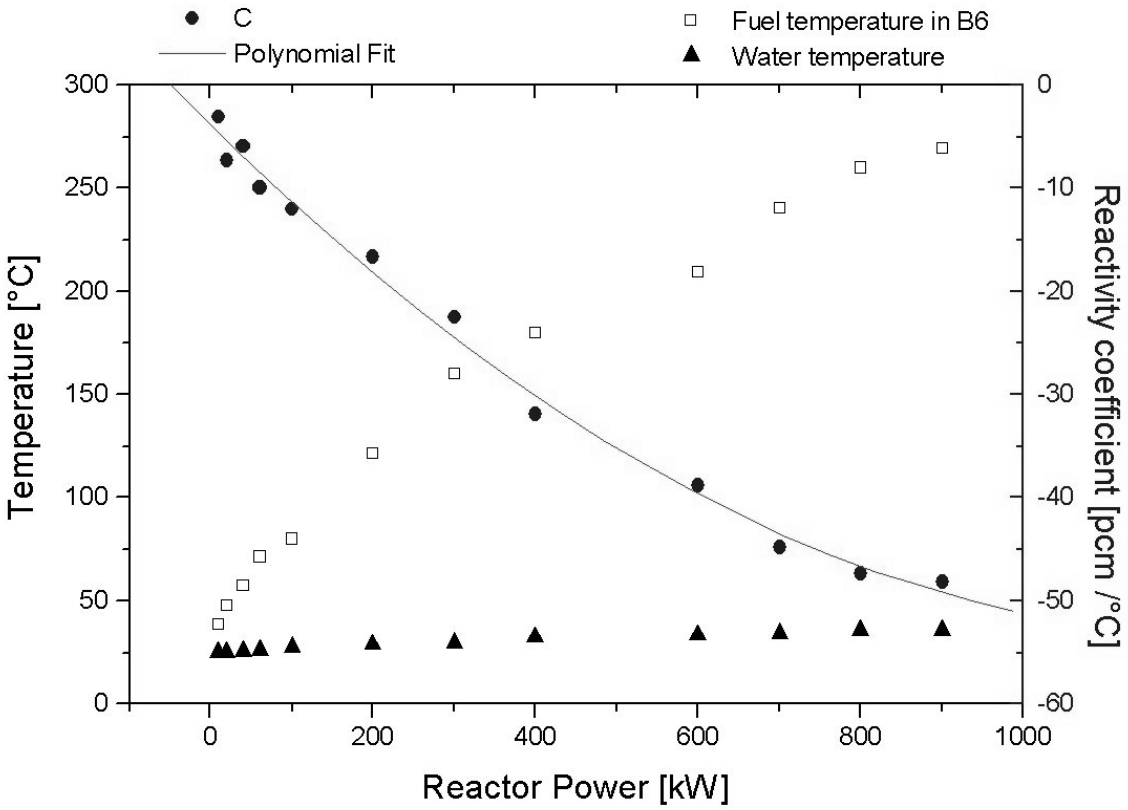

Figure 38 Fuel and water temperature with prompt temperature coefficient

References

1 M. Salvatores, A. D'Angelo and D. Naberejnev, *The demonstration of the ADS concept*, International workshop on the accelerator reliability, Santa Fe, MUSA, May 2002

2 M. Carta, and A. D'Angelo, "Subcriticality Level Evaluation in Accelerator Driven Systems by Harmonic Modulation of the External Source", Nucl. Sci. Eng., 133, 282-292 (1999).

3 D. G. Cacuci, 'On perturbation theory and reactor kinetics: from Wigner's pile period to accelerator driven systems', Int. Conf. PHYSOR 2002, Seoul, Korea, 2002

4 "TRADE Final Feasibility Report - March 2002" by the Working Group on TRADE : TRiga Accelerator Driven Experiment.

5 V. Kulik, MCNP Calculations for TRADE-TRIGA Reactor, ANL Intra-Laboratory memo, Sept. 30, 2002

6 Personal communication with ENEA, Italy, 2002

7 L. Mandard, Personal communication

8 R. V. Griffith, J. Palfalvi and U. Madnvanath, Compendium of neutron spectra and detector responses for radiation protection purposes, technical report series N. 318, IAEA, Vienna, 1990

9 J. P. Hudelot, et. al., *Calibration des chambres á EOLE/MINERVE et MASURCA dans les spectres de référence du réacteur BR1 du CEN MOL*, CEA Note Technique, 02/037, (January, 2003)

10 S. Glasstone and A. Sesonske, *Nuclear Reactor Engineering*, Chapman & Hall (1994)

11 *Technical Foundation of TRIGA*, General Atomic report (1958)

12 L. Di Palo, et. al.,*Reattore RC-1 1MW, Progetto Definitivo, Rapporto di Sicurezza (Licensing style)*, ENEA report (April, 1966)